REPORT DOCUMENTATION PAGE

AFRL-SR-BL-TR-00-

0582

1. REPORT DATE (DD-MM-YYYY) 19/11/1998	2. REPORT TYPE Final Technical Report	3. DATES COVERED (From - To) 02/28/96-03/01/99

4. TITLE AND SUBTITLE

Novel Photorefractive and Electro-optic Polymers-Rational Designs, Synthesis and Mechanism

5a. CONTRACT NUMBER

5b. GRANT NUMBER
F49620-96-1-0047

5c. PROGRAM ELEMENT NUMBER

6. AUTHOR(S)

Professor Luping Yu

5d. PROJECT NUMBER

5e. TASK NUMBER

5f. WORK UNIT NUMBER

7. PERFORMING ORGANIZATION NAME(S) AND ADDRESS(ES)

The University of Chicago,
Department of Chemistry
5735 South Ellis Avenue
Chicago, IL 60637

8. PERFORMING ORGANIZATION REPORT NUMBER

9. SPONSORING / MONITORING AGENCY NAME(S) AND ADDRESS(ES)
AFOSR/NL, 801 N. Randolph Street,
Ste 732, Arlington VA 22203-1977

10. SPONSOR/MONITOR'S ACRONYM(S)

11. SPONSOR/MONITOR'S REPORT NUMBER(S)

12. DISTRIBUTION / AVAILABILITY STATEMENT
Reproduction in whole or in part is permitted for any purpose of the United States
Government. This document has been approved for public release and sale; its distribution is
unlimited.

13. SUPPLEMENTARY NOTES

14. ABSTRACT
This report describes our effort in the past three years on synthesis and characterization of novel photorefractive polymer system. Two major systems were developed, one of which combined the ionic transition metal complexes and a conjugated polymer backbone bearing NLO chromophores to manifest large photorefractive effect. Another is a molecular material containing oligothiophene and a nonlinear optical (NLO) chromophore. A large net optical gain (>200 cm^{-1}) at a zero electric field was observed in the metal containing system. In the molecular system, a net optical gain of 83 cm^{-1} and a diffraction efficiency of nearly 40% were obtained in a film made from this molecule under an applied field of 706 kv/cm. A fast response time of for the grating formation, 42 ms under 616 kv/cm, was observed.

20001106 133

15. SUBJECT TERMS

16. SECURITY CLASSIFICATION OF: None			17. LIMITATION OF ABSTRACT	18. NUMBER OF PAGES	19a. NAME OF RESPONSIBLE PERSON Luping Yu
a. REPORT None	b. ABSTRACT None	c. THIS PAGE None		39	19b. TELEPHONE NUMBER (include area code) 773-702-8698

DTIC QUALITY INSPECTED 4

Final Technical Report

To
Air Force Office Of Scientific Research

Grant Number: **F49620-96-1-0047**

Prepared by

Professor Luping Yu

The University of Chicago
Department of Chemistry
5737 S. Ellis Avenue
Chicago, IL-60637
Phone Number: 773-702-8698
Fax number: 773-702-0805
e-mail address: lupingyu@midway.uchicago.edu

Papers published under partial sponsorship of AFSOR (F49620-96-1-0047)

1.   L. Yu, W. K. Chan, Z. H. Peng, A. R. Gharavi, "Multifunctional Polymers Exhibiting Photorefractive Effects", *Account of Chemical Research*, <u>29</u>, 13, (1996).

2.   Z. H. Peng, L. P. Yu, "Synthesis of Conjugated Polymers Containing Ionic Transition Metal Complexes", *J. Am. Chem. Soc.*, *118*, 3777, (1996).

3.   Z. H. Peng, A. Gharavi, L. P. Yu, "Rational Synthesis of Photorefractive Polymers", *Proc. SPIE -Int. Soc. Opt. Eng.*, (1996).

4.   P. A. Fleitz, R. L. Sutherland, N. S. Tang, W. J. Li, and L. P. Yu, "Z- Scan Measurements on Substituted Thiophene Oligomers', *SPIE Proceedings*, Denver, Vol. <u>2853</u>, (1996).

5.   Z. N. Bao, L. P. Yu, "Functionalized Conjugated Polymers", Annu. Tech. Conf.-Soc. Plast. Eng., 54th, 1442, (1996).

6.   W. J. Li, T. Maddux and L. P. Yu, "Synthesis and Characterization of Diblock Copolymers Containing Oligothiophenes With Defined Regiospecificity and Molecular Weights", *Polym. Preprints*, *37(2)* , 378 (1996).

7.   Z. H. Peng, A. Gharavi and L. P. Yu, "Metal Complex-Containing Polymers With Large Photorefractivity", *Polym. Preprints*, *37(2)* , 380, (1996).

8.   W. J. Li, L. P. Yu, "Syntheses of Oligothiophene with Defined Regiospecificity and Molecular Weights and Its Diblock Copolymers", *Macromolecules*, *29*, 7329, (1996).

9.   Z. H. Peng, A. Gharavi, L. P. Yu, "A Hybridized Approach to New Polymers Exhibiting Large Photorefractivity", *Appl. Phys. Lett,* *69*, 4002, (1996).

10.   L. P. Yu, W. K. Chan, Z. H. Peng, W. J. Li, A. R. Gharavi, "Photorefractive Polymers", *Invited Book chapter in "Organic Conductive Molecules and Polymers"*, Ed. H. S. Nalwa. John Wiley and Sons, New York, Vol. 4, Chapter 5, 233, (1997).

11.   T. Maddux, W. J. Li and L. P. Yu, "Stepwise Synthesis of Substituted Oligo(phenylene-vinylene) via an Orthogonal Approach", *J. Am. Chem. Soc.*,*119*, 844, (1997).

12.   Z. H. Peng, A. R. Gharavi and L. P. Yu, "Synthesis and Characterization of Photorefractive Polymers Containing Transition Metal Complexes as Photosensitizer", *J. Am. Chem. Soc.*, *119*, 4622, (1997).

13.   S. Deb; T. Maddux and L. P. Yu, "A Simple Orthogonal Approach to Polyphenylenevinylene Dendrimers", *J. Am. Chem. Soc.*, *119*, 9079, (1997).

14. W. J. Li, A. Gharavi, Q. Wang and L. P. Yu, "A Multifunctional Photorefractive Molecule Containing Oligo(3-hexylthiophene) and A Nonlinear Optical Chromophore", *Polymer Preprints, 38(2),* 508, (1997).

15. Q. Wang, Ali Gharavi, W. J. Li and L. P. Yu, "Carbazole-Based Multifunctional Molecules for Photorefractive Applications", *Polymer Preprint, 38(2),* 516, (1997)..

16. W. Zhu, W. J. Li and L. P. Yu, "Investigation of the Liquid Crystalline-Isotropic Phase Transition in Oligo(phenylenevinylene)", *Macromolecules, 30,* 6274, (1997).

17. W. J. Li, T. Maddux, L. P. Yu, "Stepwise Synthesis of Substituted Oligo(phenylene-vinylene) via an Orthogonal Approach and Their Diblock Copolymers", Submitted to J. Am. Chem. Soc..

20. Qing Wang, Liming Wang, and Luping Yu, "Synthesis and Unusual Physical Behavior of A Photorefractive Polymer Containing Tri(bispyridyl) Ruthenium(II) Complexes as Photosensitizer and Exhibitng a Low Glass-Transition Temperature", *J. Am. Chem. Soc.,* Accepted.

21. W. J. Li, A. Gharavi and L. P. Yu, "Photorefractive Molecule Containing Oligo(3-hexylthiophene) and A Nonlinear Optical Chromophore", *Adv. Mater.10,* 927, (1998).

22. Q. Wang, N., Quevada, A. Gharavi, and L. P. Yu, "Novel Photorefractive Materials Based On Multifunctional Organic Glasses", in ACS Symposium Series "Field Responsive Polymers". 1998, in press.

23. W. J. Li, A. Gharavi, Q. Wang and L. P. Yu, "A Multifunctional Photorefractive Molecule Containing Oligo(3-hexylthiophene) and A Nonlinear Optical Chromophore", in ACS Symposium Series "Field Responsive Polymers". 1998, in press.

24. L. M. Wang, Q. Wang, and L. P. Yu, "The Effect of a Local Field on Photogeneration Efficiency in a Novel Photorefractive Polymer", *Appl. Phys. Lett.,* in press.

A. Synthesis and Characterization of Photorefractive Polymers Containing Transition Metal Complexes as Photosensitizer.

Photorefractive effect involves the modulation of the index of refraction of a material by a space charge field via the electro-optic effect.[2] This space charge field arises from the redistribution of charges in a photoconductor when it is illuminated with a nonuniform light intensity pattern. Since the change of refractive index is proportional to the magnitude of the space charge field, the generation of a large space charge field is crucial for a high PR performance. The formation of a space charge field involves three processes: the generation of free charge carriers, the transport of them and eventually trapping by a trapping center. Therefore, in order to build up a large space charge field, the optimization of these three processes is essential.

In the majority of these inorganic ferroelectrics ($BaTiO_3$, $Bi_{12}SiO_{20}$ (BSO), $Sr_xBa_{1-x}NbO_3$ etc.) with a pronounced photorefractive effect, Fe^{2+}/Fe^{3+} impurities play the most important role as

electron donor and trapping centers. It is believed that the photoinduced interconversion of $Fe^{2+} <-> Fe^{3+}$ and the efficient band transporting of the free charge carriers are responsible for the buildup of space charge fields.

Unlike their inorganic counterpart, organic PR materials lack such mechanisms for the formation of the photoinduced space charge field.[1(a)] Their photogeneration of charge carrier is accomplished through exciton dissociation and free charge carriers are transported away through a hoping mechanism along a series of transporting molecules. Because of the low dielectric constant and numerous channels for the relaxation of excited states to the ground state, the quantum yield for the charge generation in organic materials is usually low. To address these problems, we recently designed a new photorefractive polymer system which contains multivalent transition metal complexes (Ru^{2+} or Os^{+2} complexes) and conjugated polymer backbones. In this system, the conjugated polymer backbone was chosen to play the dual role of both transporting channel for the charge carriers and the macroligand to chelate with the transition metal-complex.

It is well known that doped conjugated polymer systems have high electrical conductivities.[5] Although band transport theory may not be valid for the charge transporting in these systems. Charge transporting through polaron or bipolaron states which are resided in the forbidden gap could be also very efficient.[6] Therefore, conjugated backbone could provide an efficient charge transporting pathway and it could facilitate the formation of the space charge field.

Ru(II)-tri(bispyridyl) complexes were chosen as the photocharge generator. $Ru(bpy)_3^{2+}$ is known to exhibit interesting metal-to-ligand charge transfer (MLCT) process and have been extensively studied on their behavior in photochemistry, photophysics, electrochemistry, and electronic/energy transfer process.[7] They have also been extensively studied as light-harvesting materials, materials which can reduce water into hydrogen when coupled with other components.[8] To utilize their interesting charge transfer properties in the synthesis of PR polymers, Ru(II) complexes were designed to chelate with the conjugated polymer backbone. Upon excitation in the region of the MLCT transition of the Ru complex, electrons would be injected into the polymer backbone (equivalent to n-doping of PPV), transported away through either intrachain migration or interchain hopping and eventually trapped by the trapping centers which could be impurities or structural defects. We envision that the combination of the efficient MLCT process of the ruthenium complexes and the efficient charge transporting process of the conjugated backbone will lead to a higher charge separation efficiency and therefore better PR performance in this new PR polymer system. Experimental results confirmed that the incorporation of the Ru-complex into the PR polymers indeed dramatically enhanced the PR performances of the resulting polymers. This approach is versatile and has been extended to synthesize Os-complex containing PR polymers which showed photorefractivity at a wavelength in the near IR regions.

A-1. Since the targeted polymer is a multifunctional polymer which contains conjugated system, NLO chromophore and ionic transition metal complex, a reaction which can tolerate all of these functionalities and possesses high yield should be utilized for the polymerization. From our previous studies and other groups' works, the Heck coupling reaction is found to be versatile to synthesize conjugated polymers.[9] Its mild reaction condition and tolerance for a variety of functional groups are especially useful for synthesizing such functional polymers. We have previously demonstrated that the Heck coupling reaction can be utilized to synthesize conjugated polymers containing ionic transition metal complexes and the resulting polymer showed enhanced photoconductivity.[10] That work is the bases for the design of our new PR polymers.

Synthesis of the monomers and polymers: To utilize the Heck reaction, Ru-complexes bearing diiodofunctional groups were synthesized according to Scheme 1 where the 5,5'-dimethyl 2, 2'-bipyridine was synthesized by the Raney nickel catalyzed self-coupling of 3-picolines. Compound **6**, a crucial compound for this approach, was synthesized by reacting compound **5** with 1 eq. butyllithium and subsequent quenching by DMF. The Horner-Wittig-Emmons (HWE) reaction between compounds **3** and **6** yielded compound **7**. The final ruthenium (or Osmium) complex (monomers **A** or **B**), soluble in common organic solvents, was prepared after refluxing the compound **7** with Ru(bipy)$_2$Cl$_2$ (or Os(bipy)$_2$Cl$_2$) and can be easily purified by recrystalization from THF/Hexane.

Scheme 1. Synthesis of the Ru(or Os)-complex (monomers A and B).
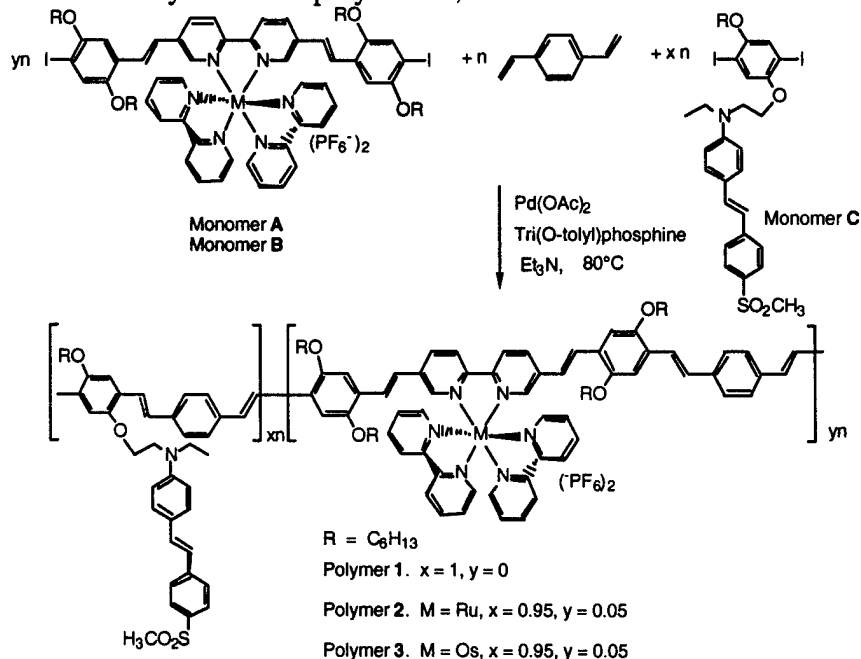

Monomer A: M = Ru.
Monomer B: M = Os.
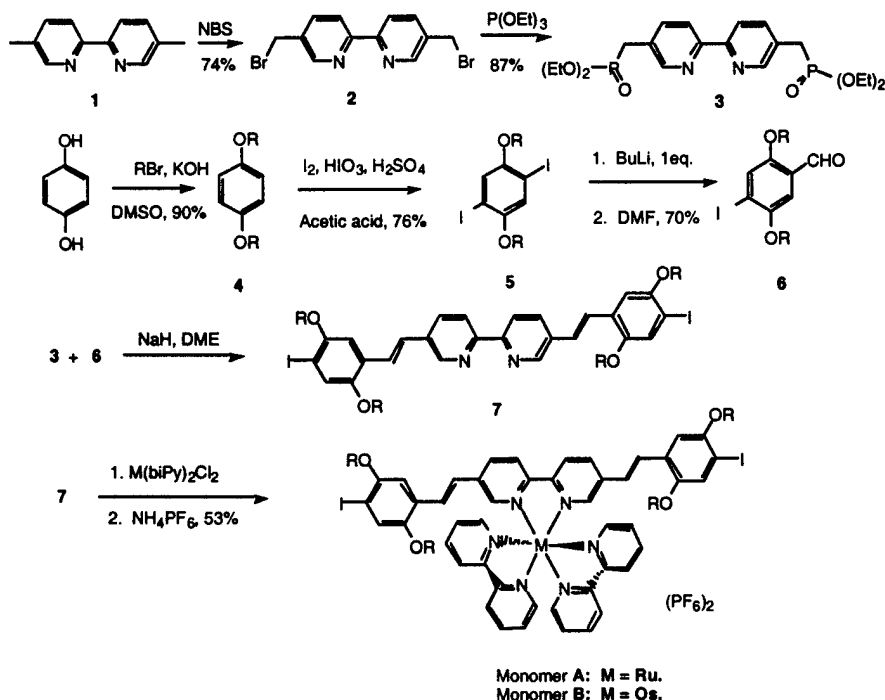
Monomer **C** was synthesized by using the approach outlined in Scheme 2. This monomer contains an alkoxyl substitutent which was introduced to increase the solubility of the resulted conjugated polymers; the polymer without this substitutent was insoluble in common organic solvents due to the strong interchain π-π interactions.

5

Scheme 2. Synthesis of monomer B.
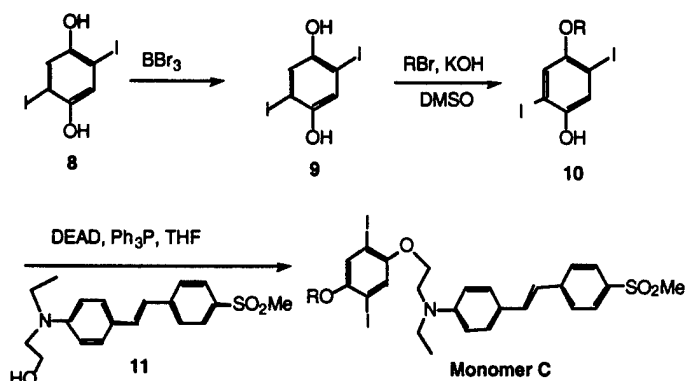
The polymerization was carried out according to Scheme 3 where the Pd(OAc)$_2$/P(o-tolyl)$_3$/NEt$_3$ (0.04 : 0.2 : 2.5 mol ratio relative to divinyl benzene) was applied as the catalytic systems. Polymers soluble in tetrachloroethane, DMF, NMP were obtained in excellent yields.

Scheme 3. Synthesis of polymers **1**, **2** and **3**.

R = C$_6$H$_{13}$
Polymer 1. x = 1, y = 0
Polymer 2. M = Ru, x = 0.95, y = 0.05
Polymer 3. M = Os, x = 0.95, y = 0.05

Structural characterization: Polymers **1** and **2** are insoluble in THF, chloroform but soluble in tetrachloroethane (TCE), DMF, NMP etc. Their intrinsic viscosities were measured to be 0.46, and 0.53 dL/g, respectively, in NMP at 30°C, indicating that reasonable high molecular weights were obtained. Good optical quality films with thickness over 30 μm can be casted from their TCE solutions.

The ^{1}H NMR spectra of polymers **1** and **2** in tetrachloroethane-d$_4$ were very similar to each other. The major peaks are corresponding to the protons of the chromophore and the divinyl benzene moieties. However, the chemical shifts due to the protons of the bipyridyl ligand at 8.0 and 8.5 ppm

6

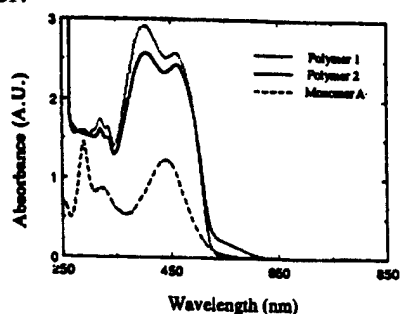are still noticeable for polymer **2**, indicating the incorporation of the ruthenium complex into the polymer.

Figure 1.   UV/Vis spectra of monomer **A** and polymers **1, 2**.

The UV-Vis spectra of the polymers are shown in Figure 1. Both polymers **1** and **2** exhibit two major peaks: one at 390 nm which is due to the absorption of the NLO chromophore, the other at 460 nm which is attributed to the absorption of the conjugated backbone. For polymer **2**, however, there is an absorption tail extending beyond 600 nm, which can be assigned to the metal-to-ligand charge transfer absorption of the ruthenium complexes. This is a further evidence for the incorporation of the ruthenium complex into the polymer. It also indicates that the incorporation of the ruthenium complex extends the photosensitivity of the polymer to the region of longer wavelengths. By using diode laser (i.e. 690 nm), we can photoexcite the polymer mainly through the MLCT process while the absorptions due to the NLO chromophore and the conjugate backbone can be minimized. It can be noted that a small peak at 290 nm, due to the ligand-centered transition of the two bipyridyl ligand in the ruthenium complexes, exists for polymers **2** while polymer **1** does not have this absorption.

DSC studies showed that polymers **1** and **2** had a similar glass transition temperature at ca. 130 °C. The main chain melting temperature for polymers **1** and **2** was observed at 215 °C, which overlapped with the crosslinking temperature of the conjugated polymer backbone.[13] TGA analysis showed that polymer **1** was stable up to 350 °C while polymers **2** has a small weight loss starting at 270 °C, caused by the loss of the bypyridyl ligands in the ruthenium complexes.

Physical Characterization: The second-order nonlinearity of the poled polymers was demonstrated by the second harmonic generation (SHG) measurement. After corona poling, a SHG coefficient, d_{33}, of 70 pm/V for polymer **2** was obtained at 1064 nm. The poled polymer films also exhibited reasonable thermal and temporal stabilities in their optical nonlinearity. It was found that the SHG signal of polymer **2** was stable up to 80 °C. When the poled polymer film was kept at 60 °C, the SHG signal, after an initial drop, stabilized at an value of 80%. This stability of the nonlinearity allowed us to perform the photorefractive experiments without applying an external electric field.

To further demonstrate the electro-optic effect, the EO coefficient of polymer **2** was measured using a reflection method.[14] An E-O coefficient of 7 pm/V was obtained at 690 nm, a quite high value as compared to other photorefractive polymers. This large nonlinearity arises from the large NLO chromophore composition in the polymers (~70 wt %).

The photoconductivity of the polymers, another necessary condition for PR effect, was measured at a wavelength of 690 nm. As expected, polymer 2 exhibited large photoconductivity. A photoconductivity of 3×10^{-10} Ω^{-1} cm^{-1}/(W/cm^2) and a photocharge generation efficiency of 0.2%

7

were obtained under an external electric field of 950 kv/cm. This value is a significant improvement from our previous polymers.[15]

To study the PR effect, a most effective technique is the two beam coupling experiment which is regarded as the standard experiment to confirm the PR response. We performed the two beam coupling experiment at 690 nm (diode laser, s-polarized). The normal of the sample was rotated 35° with respect to the bisector of the writing beams to obtain a non zero projection of the EO coefficient. The transmitted beam intensities were measured with lock-in amplifiers (time constant of the lock-in amplifiers was set at 10 ms) and the data was collected by a computer. At the time of 20 seconds, the two laser beams were overlapped at a pristine spot inside the polymer film. Notice that the intensity of one beam, as a function of time, kept on increasing while that of the other decreasing. The gain and loss was calculated (the ratio of the two incident beam intensities is 1.12) by the following equation: $\Gamma = \frac{1}{L}\ln(\frac{1+\alpha}{1-\beta a})$; where α is the ratio of the intensity modulation

$\Delta Is/Is$); β is the intensity ratio of the two incident laser beams (Is/Iq). It was found that polymer **2** exhibited an optical gain higher than 300 cm^{-1}. At the time of 700 seconds, the pump beam was blocked and the transmitted intensity of the other beam went back to the initial value. When the sample was rotated 180 °C along its axis, the gain and the loss beams were switched due to the reversion of the dipole orientation. This result clearly showed that the grating was indeed of photorefractive nature, although the process is rather slow.

By utilizing a known technique,[16] the phase of index grating can be studied. This experiment can furnish further evidences for the photorefractive effect. After forming the grating by intersecting the two laser beams inside the polymer film for a few minutes, the sample plate was translated along the direction parallel to the grating wave vector. The transmitted intensities of the two beams exhibit an oscilating pattern which reflect the spacing and phase of grating. It was shown that a 90° phase shift of the index grating over the intensity distribution exists for polymer **2.** This result verified the photorefractive nature of the grating. Since polymer **2** exhibits an absorption coefficient of 102 cm^{-1}, a large net optical gain was obtained in this polymer at a zero external electric field.

Synthesis of Near IR Sensitive PR polymers: The synthetic approach described above is versatile and can be applied to synthesize other metal-containing polymers, such as polymers containing Os-complexes. The advantage to utilize Os-complex as the photosensitizer is that Os-complex has a spin allowed ^{1}MLCT transition at 450 nm and an extremely broad (over 200 nm bandwidth) spin forbidden ^{3}MLCT transitions at around 640 nm (see Figure 5, the UV/vis spectrum for Monomer B).[ref.] The broad absorption which extends beyond 750 nm is very useful for the design of IR sensitive materials. If we polymerize the Os-complex into the conjugated PR polymer system, the resulted polymer could show photorefractivity at wavelengths in the near-IR regions (for example at 780 nm).

The Os-complex (Monomer **B**) was synthesized by reacting the ligand (Compound **7** in Scheme 1) with Os(II)(bpy)2Cl2, which was prepared according to a literature procedure.[17] The resulted Os-complex is black shining powder, which is soluble in common organic solvents such as chloroform, THF, methylene chloride etc.

For a comparison, a polymer with the same molar composition (5 mol % Os-complex) as polymer **2** was synthesized (Polymer **3**) by using the Heck reaction at similar conditions. Polymer **3** is a dark powder which is soluble in NMP, DMF etc. The incorporation of the Os-complex into the polymer backbone can be clearly seen from its UV/vis spectrum. As shown in UV/vis spectrum,

8

there is an absorption tail extending to 600 nm, which can be assigned to the spin allowed transition of the Os-complex Figure 3. The inset of Figure 6 was the UV/Vis spectra of concentrated polymer solutions. It can be clearly seen that polymer **3** has an absorption tail extending to near 800 nm.
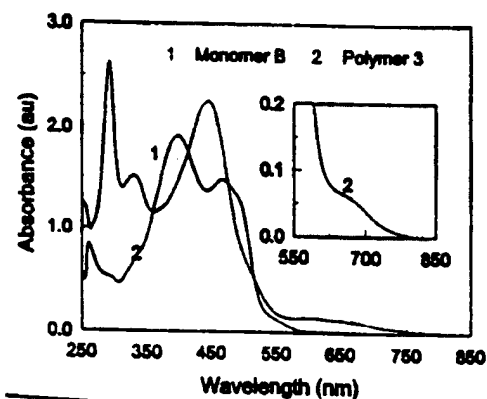

Figure 2. UV/Vis spectra of the Os-complex (in THF solution).

The polymer has a glass transition temperature of 110 °C and a crosslinking temperature of 175 °C. TGA analysis showed two weight losses, one started at 240 °C and the other at 310 °C. The first weight loss (6%) is due to the decomposition of the Os-complex while the second one is due to the decomposition of the backbone.

Two beam coupling experiment was performed at 780 nm (30 mW, s-polarized). A polymer film with a thickness of 5.09 μm was prepared. The sample was tilted 30° and the angle between the two incident laser beams was 46.4°, which gave a grating spacing (Λ) of 0.24 μm (the polymer has a refractive index of 1.7486 at 780 nm). The data was taken under a zero external field after overlapping the two laser beams inside the sample for four to five minutes. The asymmetric energy exchange was clearly observed. The corresponding optical gain was calculated to be 80.4 cm^{-1}. Although net optical gain was not realized (α was measured to be 186 cm^{-1}), the observation of such a photorefractive reponse at near IR region is still very interesting. Net optical gain may be obtainable for polymers with less Os-complex concentrations.
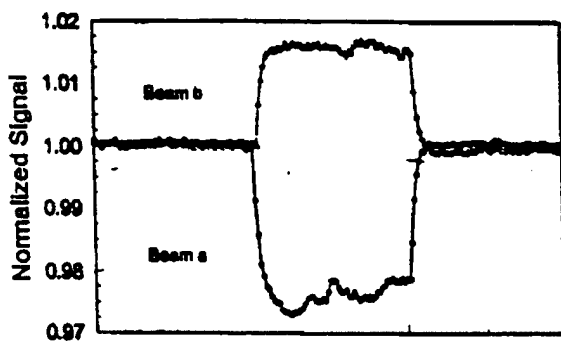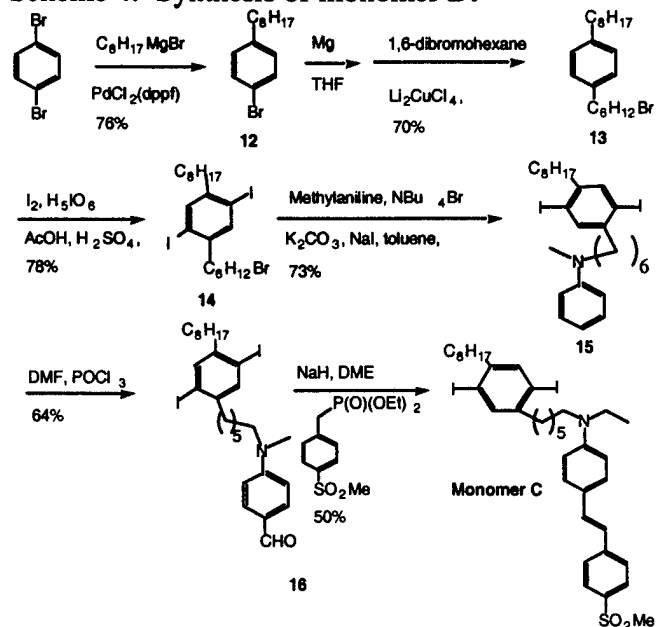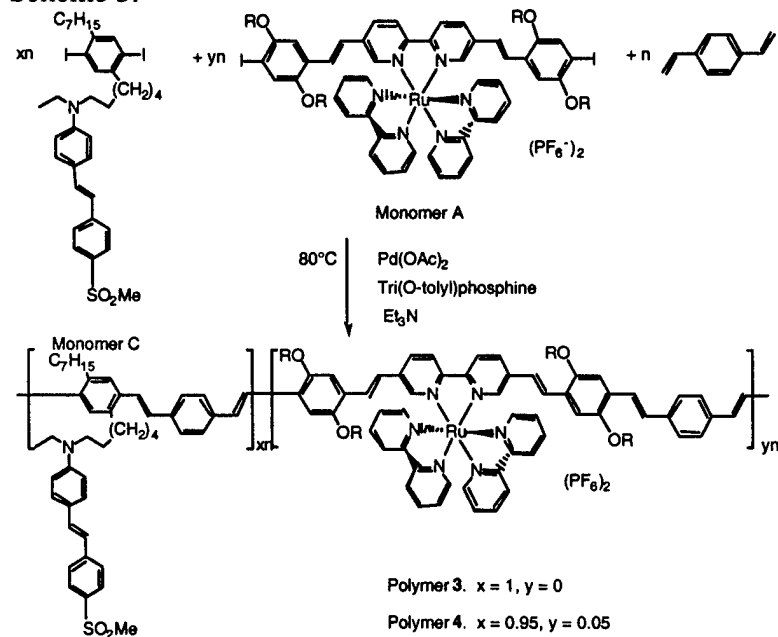

Figure 3. Asymmetric energy exchange in the 2BC experiment for polymer **5** at zero external field.

Scheme 4. Synthesis of monomer D.

Scheme 5.

Polymer 3. x = 1, y = 0
Polymer 4. x = 0.95, y = 0.05

PR Polymers Based on Alkyl-Substituted PPV: As mentioned earlier, the alkoxy-substituted PPV has a π-π* transition at a maximum of 450 nm, which is still partially overlapped with the MLCT transition of the Ru-complexes. It is understandable that any absorption at the working laser wavelength (690 nm in our case for Ru-complex containing polymers) by the component other than the photocharge generator is a waste of photons and should be minimized. It is known that the π-π* transition of alkyl-substituted PPVs occurs at shorter wavelengths. If we can change the alkoxy substitutes in polymer 2 to alkyls, we should be able to decrease the absorption of the PPV backbones significantly. For this purpose, a new chromophore (monomer **D**) was

synthesized as shown in Scheme 4. The polymer structures were shown in Scheme 5. Two polymers were synthesized: polymer **4** without Ru-complex and polymer **5** with 5 mol % Ru-complex.

Unlike polymers **1** and **2**, polymers **4** and **5** are soluble in chloroform and THF. Their molecular weights were measured to be 21 kdalton (Mn, PD = 2.8) and 18 kdalton (Mn, PD = 2.25), respectively, by GPC (polystyrene as standard). The incorporation of the Ru-complex into the polymer backbone was again proved by the ^{1}H NMR spectra, typical chemical shifts at 8.0 and 8.5 ppm due to the bipyridyl ligand protons and at 4.0 ppm due to the -OCH$_2$- protons was observed for polymer **5**.

The UV/Vis spectra of the polymers showed that the absorption due to the PPV backbone overlapped with that of the chromophores, both with a maximum at around 380 nm. Again, polymer **5**, unlike polymer **4**, has an absorption tail extending beyond 600 nm. Since both the chromophores and the PPV backbones essentially have no absorption beyond 500 nm, much smaller absorption coefficient (21.5 cm^{-1}) was obtained for polymer **5**.

Polymers **4** and **5** have a relatively low glass transition temperature of 75 °C. Consequently their SHG stability are not as good as polymers **1** and **2**. However, we were able to prepare thick films sandwiched between two ITO coated glasses. As shown in Figure 3, when an electric field (1000 v over 75 μm thick film) was applied at 20 seconds, the transmitted intensity of one beam increased while that of the other beam decreased with a response time of 10 seconds. Energy exchange of more than 5% between the two beams was observed , which gave an optical gain of 16 cm^{-1}. When the field was turned off at 60 seconds, the intensities of the two beams went back to their original values gradually in 20 seconds. This results demonstrated its photorefractivity. Considering the small field applied (less than 15 V/μm), one would expect higher optical gain values if higher electric fields could be applied.
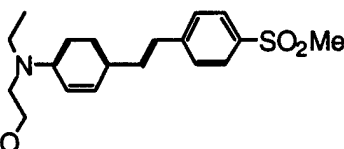
Study of the structural defects in the Heck reaction and their effects on the photorefractivity: It was found that the ^{1}H NMR spectra of all of our polymers synthesized by the Heck reaction exhibited small peaks which cannot be removed by any purification process. For example, as shown in Figure 1, multiple peaks between 0.90~1.35, 6.52 and a peak at 3.73 ppm exist. It is known that the Heck reaction involved many side reactions which clearly will introduce defects into the conjugated backbone.[18] These defects may play the role of deep trapping centers and thus exert profound effect on the PR performance of the polymers. To identify the structural defects in the conjugate polymers synthesized by the Heck reaction, we carried out model reactions involving similar monomers and styrene as shown in Scheme 6.

**Scheme 6.** Model reactions via the Heck coupling.
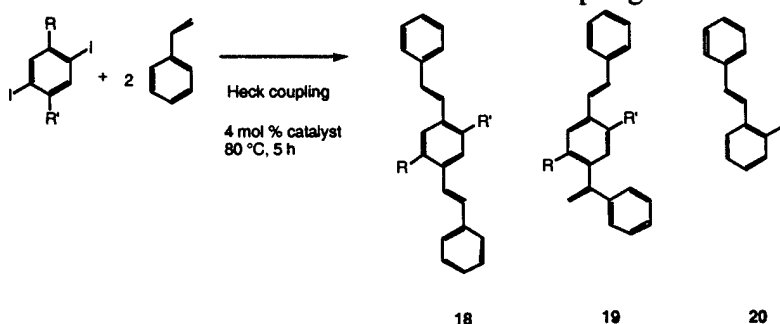
Three diiodo compounds were used to run the model reactions. After completion of the reaction, the mixtures were poured into aqueous solution (5% HCl) and extracted with ethyl ether. The ^{1}H NMR spectra of the mixture were collected. Based on that, the relative yields of the products were calculated. The results were shown in Table I.

Table I. Yields of the products in the model reaction.

Entries	R	R'	18	19	20
a	OC_6H_{13}	OC_6H_{13}	85	14	1
b	C_6H_{13}	C_6H_{13}	92	8	---
c	OC_7H_{15}	(structure with $-SO_2Me$)	90	10	---

Within 5 hours, the coupling reactions completed for all of three model reactions (no proton peaks corresponding to the diiodo-starting material were observed in the ^{1}H NMR of the reaction mixture). It was found that a significant amount of α-substituted product **19** were obtained in all three cases. The small peaks mentioned above in the ^{1}H NMR spectra of polymers correspond well to the α-substituted structural moieties. These α-substituted units break the conjugation and therefore form stuctural defects. However, the integrations of the peaks of these defects in the ^{1}H NMR spectra of polymers are much smaller than that observed in the model reactions although the exact reason is not very clear.

Scheme 7. Synthesis of monomer E.
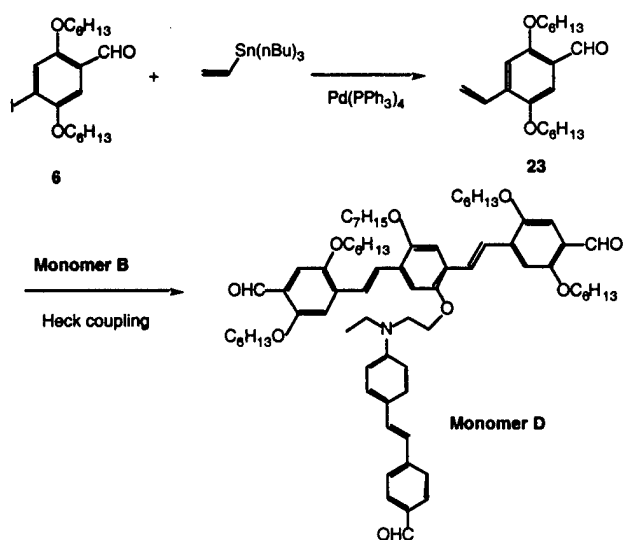
To study the effect of these defects on the polymer properties, we synthesized two conjugated polymers with the same chemical structure by different approaches. As shown in scheme 8, while polymer 7 was synthesized through the Horner-Wittig-Emmons (HWE) reaction.

It is known that tetraethyl xylylenebisphosphonate (compound 22) reacts with benzaldehyde resulting in only trans products.[10] In addition, the phosphorus product is a phosphate ester and hence soluble in water, which makes it easy to separate it from the olefin product. We found that HWE reaction gave all-trans linear conjugated polymers.

Scheme 9. Synthesis of polymers 8 and 9 via HWE reaction.
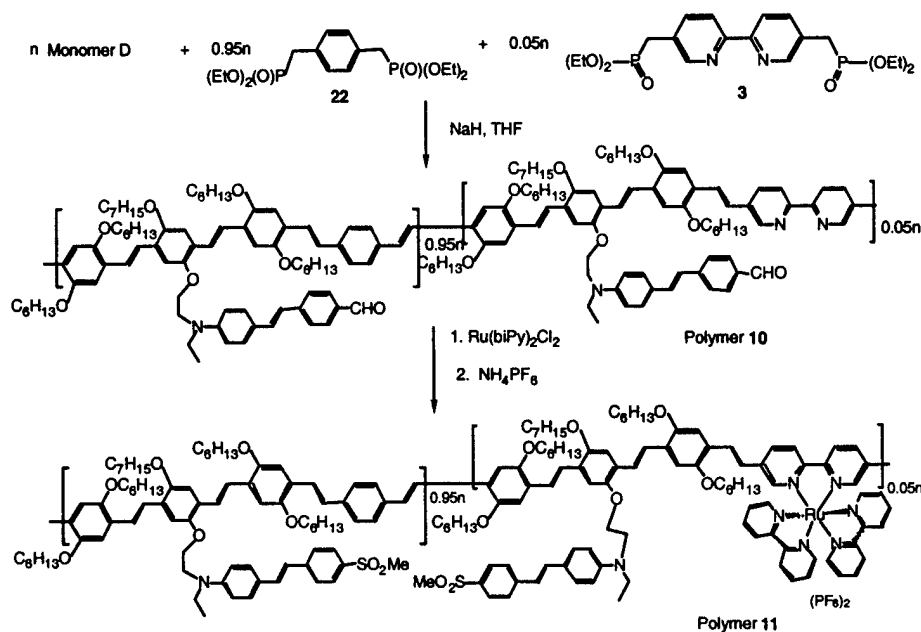
Polymer 6 (Mw = 34 kdalton, intrinsic viscosity = 0.48 dL/g) has a brown color and is soluble in THF, DMF, NMP etc. while polymer 7 (intrinsic viscosity = 0.56 dL/g) was red-colored and insoluble in THF, partially soluble in DMF, NMP etc.

The ^{1}H NMR spectra of the polymers clearly showed that polymer 7 has less structural defects than polymer 6 (Figure 10). The side peaks corresponding to the α coupling structures were observed at 1.02, 1.10, 1.18, 3.74, 5.3, 5.6 ppm for polymer 6 but not for polymer 7. The UV/Vis spectrum of polymer 7 shows an absorption maximum at 465 nm, a 10 nm red shift compared to that of polymer 6, which could imply a better conjugation in polymer 7.

More significant difference came from the thermal properties of these two polymers. As shown in the DSC studies (Figure 11), polymer 7 has a clear backbone melting transition at 270°C and is stable upto 350°C, while polymer 6 shows a broad melting transition at 200°C and starts to decompose at 300°C. These results clearly demonstrate that the bulky properties of the polymers depend strongly on the synthetic approaches. Polymer 7 synthesized by the HWE reaction has more regular linear trans structure and therefore higher crystallinity, and longer absorption maximum.

As a further step, we synthesized the ruthenium complex containing PR polymers via the HWE reaction. As shown in Scheme 8, we utilized the Heck reaction to synthesize monomer E from monomer C. Considering the uncertainty of the Ru-complex under the harsh reaction condition of the HWE reaction (strong base was used), we chose to synthesize the conjugate

13

polymer first and then coordinate with the ruthenium complex. This approach, of course, lacks the certainty about the yield of the coordination of the ruthenium complexes.

As shown in scheme 9, polymer **8** was synthesized as a red powder. THF was found to be the best solvent for the polymerization and the polymer precipitated out of the reaction mixture in several hours. The final coordination step was carried out in THF. The resulted polymer **9** showed much better solubility in THF, chloroform etc. than polymer **8**.

The ^{1}H NMR spectra of the two polymers (**8** and **9**) showed no clear difference. But UV/Vis spectra do provide some structural information. As shown in Figure 12, polymer **9** showed a backbone absorption maximum at 474 nm, slightly blue-shifted compared to polymer **8** (477 nm), and an absorption tail extending near 600 nm. These results imply that some coordination of the ruthenium complex indeed occurred. Another evidence of the coordination comes from the elemental analysis, 0.09% of ruthenium was found in the polymer, which accounts for 12% of the dipyridyl site. This low coordination ratio could be due to the poor solubility of polymer **8**.

Preliminary two beam coupling studies showed encouraging results. As shown in Figure 13, a response time of 150 seconds and an optical gain of 99 cm^{-1} were obtained. Indeed, the photorefractive response time is faster than our previous PR polymers made by the Heck reaction (over 500 seconds), although the comparison should be cautious. The smaller optical gain could be due to the incomplete coordination of the ruthenium complexes

Conclusions

We have demonstrated that the hybridized polymers which combined the ionic transition metal complexes and a conjugated polymer backbone bearing NLO chromophores exhibited large photorefractivity. In this system, the conjugated polymer backbone was designed to play the dual role of both transporting channel for the charge carriers and the macroligand to chelate with the transition metal-complex. Ru(II)-tri(bispyridyl) complexe was selected as the photocharge generator because of its metal-to-ligand charge transfer properties. The Heck coupling reaction was successfully applied to synthesize these multifunctional polymers. A large net optical gain (>200 cm^{-1}) at a zero electric field was observed. The synthetic approach is versatile and was extended to the synthesis of PR polymers containing Os-complexes. The resulted polymer showed photorefractivity at a wavelength in the near IR region, which is the first example of IR sensitive PR polymers. This approach also offers opportunity to fine-tune the electronic properties of polymers through easy modification of the polymer structures. Model reactions were studied to elucidate the structural defects caused by the side reactions in the Heck reaction. The effects of these defects on the PR performance of these polymers were evaluated. It was demonstrated that elimination of these defects could enhance the photorefractive response time. This work also indicated a dilemma in choosing polymerization approaches: the Heck reaction introduces undesired structural defects in the conjugate backbone. However, it can unambiguously assure the coordination of the transition metal complex, while HWE reaction does in the opposite way. Therefore, a new polymerization method which can not only tolerate transition metal complex, but also give defect-free linear conjugate polymer chain is needed.

Experimental Section

THF and Ethyl ether were purified by distillation over sodium chips and benzophenone. Styrene was distilled over calcium hydride. The p-divinyl benzene was separated from a mixture of

p-divinylbenzene and m-divinylbenzene according to the literature procedure.[20] All of the other chemicals were purchased from Aldrich Chemical Co. and used as received unless otherwise stated.

Syntheses of monomers: The following compounds were synthesized according to literature procedures: 5,5'-dimethyl-2,2' bipyridine **1**,[21] compound **2**,[16] compound **5**.[11]

Compound 3. The mixture of compound **2** (3.00 g, 8.77 mmol) and P(OEt)$_3$ (4.37 g, 26.3 mmol) was stirred at 125 °C for 4 hours. The excess amount of P(OEt)$_3$ was distilled out and the residual solid was recrystallized from chloroform/hexane to give 3.50 g of compound **3** (87%, m.p. 99-100 °C). ^{1}H NMR (CDCl$_3$, ppm): δ 1.27 (m, 12 H, -CH$_3$), 3.16 (d, J = 21.71 Hz, 4 H, -CH$_2$-P-), 4.03 (m, 8 H, -OCH$_2$-), 7.73 (d, J = 8.16 Hz, 2 H, aromatic protons), 8.27 (d, 8.07 Hz, 2 H, aromatic protons), 8.50 (s, 2 H, aromatic protons). Anal. Calcd for C$_{20}$H$_{30}$N$_2$O$_6$P$_2$: C, 52.63; H, 6.62; N, 6.14. Found: C, 52.44; H, 6.54; N, 6.07.

Compound 6. The BuLi (14.33 ml, 2.5 M solution in hexane, 35.82 mmol) in ether (50 ml) was added dropwise into an ether solution containing 2, 5 - dialkoxy 1, 4-diiodo benzene (R = C$_7$H$_{15}$, 20.00 g, 35.82 mmol, 75 ml ether) at 0 °C. After the completion of the addition of BuLi, DMF (3.93 g, 53.76 mmol) in 15 ml of ether was added dropwise into the solution. The resulting mixture was stirred at room temperature for 2 hours, and was then poured into water (200 ml). The ether layer was washed three times with water and dried over MgSO$_4$. The ether was then removed by vacuum evaporation. The resulting liquid was dissolved in hexane and stored in a refrigerator. Compound **6** crystallized out of the solution (10.70 g, 65% yield, mp 51.5-52°C). ^{1}H NMR (CDCl$_3$, ppm): δ 0.89 (t, J = 6.56 Hz, 6 H, -CH$_3$); 1.31 (m, 8H, -CH$_2$CH$_2$-CH$_3$); 1.36 (m, 4H, -CH$_2$CH$_2$CH$_2$CH$_3$); 1.46 (m, 4 H, -CH$_2$CH$_2$CH$_2$CH$_2$CH$_3$); 1.80 (quartet, J = 6.89 Hz, 4H, -OCH$_2$CH$_2$-); 3.97 (t, J = 5.47 Hz, 2 H, -OCH$_2$-); 3.99 (t, J = 5.65 Hz, 2 H, -OCH$_2$-); 7.14 (s, 1 H, aromatic proton, ortho to CHO); 7.4 (s, 1 H, aromatic proton, meta to CHO); 10.34 (s, 1H, -CHO). ^{13}C NMR (CDCl$_3$, ppm): 14.2, 22.8, 26.1, 29.2, 29.3, 31.9, 69.6, 70.0, 108.9, 124.6, 125.3, 152.3, 155.9, 189.2. Anal. Calcd for C$_{21}$H$_{33}$O$_3$I: C, 54.79; H, 7.22; I, 27.56. Found: C, 54.86; H, 7.21; I, 27.49.

Compound 7. Sodium hydride (0.24 g, 9.81 mmol) was added to a solution of compound **6** (3.01 g, 6.65 mmol) in DME (20 ml). The resulting suspension was stirred for 5 minutes. Compound **3** (1.49 g, 3.27 mmol) in DME (10 ml) was then added dropwise at room temperature. The mixture was refluxed overnight. After the solution cooled down to room temperature, water was added. The resulting mixture was stirred for 5 minutes and the crude product was separated by filtration. Recrystalization from dichloromethane/methanol gave 2.20 g of pure compound **7**. (83%, m.p. 84-85 °C). ^{1}H NMR (CDCl$_3$, ppm): d 0.9 (m, 12 H, -CH$_3$); 1.3-1.9 (m, 40H, aliphatic protons); 3.95 (t, J = 6.2 Hz, 4 H, -OCH$_2$-); 4.01 (t, J = 6.2 Hz, 4 H, -OCH$_2$-); 6.99 (s, 2 H, aromatic protons meta to Iodo); 7.10 (d, J = 16.47, 2 H, vinyl protons); 7.26 (s, 2 H, aromatic protons ortho to Iodo); 7.44 (d, J = 15.56 Hz, 2 H, vinyl protons); 7.92 (**dd, J = 8.42 (1.73) Hz**, 2 H, 4-pyridine protons); 8.34 (d, J = 8.24 Hz, 2 H, 3-pyridine protons); 8.71 (s, 2 H, 2-pyridine protons). ^{13}C NMR (CDCl$_3$, ppm): 14.4, 22.8, 26.3, 29.3, 29.5, 32.0, 69.6, 70.3, 86.9, 110.0, 120.9, 123.7, 125.5, 126.8, 133.4, 148.3, 151.6, 152.3, 154.6. Anal. Calcd for C$_{54}$H$_{74}$N$_2$O$_4$I$_2$: C, 60.67; H, 6.98; N, 2.62. Found: C, 60.90; H, 6.93; N, 2.59.

Monomer A. A solution of 0.1500 g of compound **7** (0.14 mmol) in 10 ml of methoxyethanol was heated to 100 °C. Cis-dichlorobis(2,2'-bipyridine)ruthenium(II) hydrate (0.0679 g, 0.14 mmol) in ethanol (10 ml) was added. The ethanol was then evaporated and the

15

resulting solution was stirred at 140 °C for 3 hours. After cooling down to room temperature, the solution was added into a solution of $(NH_4)PF_6$ (0.2283 g) in water (50 ml). An orange solid was collected by filtration and recrystallized from THF/hexane to give 0.1300 g of the desired product. (53%, m.p. 234-235 °C). ^{1}H NMR (CDCl$_3$, ppm): d 0.86 (t, J = 6.56 Hz, 12 H, -CH$_3$); 1.28-1.78 (m, 40 H, aliphatic protons); 3.87-4.01 (m, 8H, -OCH$_2$-); 6.93 (d, J = 16.45 Hz, 2 H, vinyl protons); 7.07 (s, 2 H, aromatic protons meta to iodo); 7.20 (s, 2 H, aromatic protons ortho to iodo); 7.38 (d, J = 16.44 Hz, 2H, vinyl protons); 7.47 (t, J = 6.63 Hz, 2H, aromatic protons on the dipyridine ligand); 7.51 (t, J = 6.22 Hz, 2 H, aromatic protons on the dipyridine ligand); 7.67 (s, 2 H, aromatic protons); 7.81 (d, J = 5.28 Hz, 4 H, aromatic protons); 7.91 (m, 4 H, aromatic protons); 8.07 (d, J = 8.47 Hz, 2 H, aromatic protons); 8.15 (d, J = 8.67 Hz, 2 H, aromatic protons); 8.22 (t, 7.82 Hz, 2 H, aromatic protons);. Anal. Calcd for $C_{74}H_{90}N_6O_4I_2P_2F_{12}Ru$: C, 50.14; H, 5.12; N, 4.74; I, 14.32. Found: C, 50.17; H, 5.15; N, 4.73; I, 14.44.

Compound 9. To a solution of 2,5-dimethoxy 1,4-diiodobenzene (10.00 g, 25.6 mmol) in dichloromethane (50 ml), cooled in dry ice/acetone, was added dropwise the BBr$_3$ (26.50 g, 105.8 mmol) in dichloromethane (15 ml). The resulting solution was stirred at room temperature overnight and then poured into ice water. The white precipitate was collected by filtration and recrystalized from THF/hexane to yield compound **9** (8.1 g, 87%, m.p. 192-194 °C). ^{1}H NMR (CDCl$_3$, ppm): δ 7.10 (s, 2 H, aromatic protons); 9.72 (s, 2 H, -OH).

Compound 10. To the solution of compound **9** (7.00 g, 19.34 mmol) in DMSO (50 ml), potassium hydroxide powder (3.25 g, 58.02 mmol) was added. A solution of bromohexane (3.19 g, 19.34 mmol) in DMSO (10 ml) was then added immediately. The resulting mixture was stirred at room temperature overnight and then poured into water. The white solid (mainly dialkoxy-side product) was filtered out and the filtrate was neutralized by hydrochloric acid. Product was collected by filtration and further recrystalized from hexane (refrigerate) to give compound **10**.(5.00 g, 56%, m.p. 48-50°C). ^{1}H NMR (CDCl$_3$, ppm): δ 0.91 (m, 3 H, -CH$_3$); 1.34-1.80 (m, 8 H, aliphatic protons); 3.88 (t, J = 6.16 Hz, 2 H, -OCH$_2$-); 4.88 (b, 1 H, -OH); 6.97 (s, 1 H, aromatic protons ortho to OH); 7.35 (s, 1 H, aromatic protons meta to OH).

Monomer C. Diethy azodicarboxylate(DEAD) (1.0 0g, 5.7 mmol) in THF (5 ml) was added into a solution of compound **10** (1.70 g, 3.8 mmol), 4-(2-hydroxy ethyl) ethyl amino-4'-sulphone stilbene (compound **11**, 1.30 g, 3.8 mmol) and triphenyl phosphine (1.50 g, 5.7 mmol) in THF (20 ml). The resulting mixture was stirred overnight and then concentrated to less than 5 ml. The solution was poured into hot methanol and filtered while it was still hot. The resulting yellow solid was purified by chromatography (CH$_2$Cl$_2$ as eluent) and then recrystallized from acetone/methanol.

The resulted product was light yellow-colored crystal.(2.05 g, 70%, m.p.145-147 °C). ^{1}H NMR (CDCl$_3$, ppm): δ 0.90 (m, 3H, -CH$_3$ in alkoxy); 1.23 (t, J = 7.01 Hz, 3 H, -CH$_3$ on chromophore), 1.33-1.79 (m, 8H, aliphatic protons), 3.03 (s, 3H, -SO$_2$CH$_3$), 3.56 (m, 2H, N-CH$_2$-CH$_3$), 3.78 (m, 2H, -CH$_2$-CH$_2$-N), 3.90 (m, 2H, -OCH$_2$- on alkoxy side chain), 4.07 (t, J = 5.46 Hz, 2H, -OCH$_2$-CH$_2$N-), 6.69 (d, J = 8.34 Hz, 2H, aromatic protons), 6.86 (d, J = 16.33 Hz, 1H, vinyl proton), 7.12 (s, 1H, aromatic protons), 7.13 (d, J = 16.56 Hz, 1H, vinyl proton), 7.37 (d, J = 8.59 Hz, 2H, aromatic protons), 7.55 (d, J = 8.26 Hz, 2H, aromatic protons), 8.01 (d, J = 7.91 Hz, 2H, aromatic protons). ^{13}C NMR (CDCl$_3$, ppm): 12.6, 14.4, 22.8, 26.2, 29.2, 29.3, 32.0, 44.9, 46.0, 49.6, 68.1, 70.5, 86.2, 86.5, 112.0, 121.8, 122.7, 122.9, 124.3, 126.5, 127.9, 128.8, 132.9, 137.7, 144.0, 148.0,

16

152.6, 153.5. Anal. Calcd for $C_{31}H_{37}NO_4SI_2$: C, 48.13; H, 4.82; N, 1.81. Found: C, 48.22; H, 4.78; N, 1.77.

Monomer B. To the solution of compound **7** (0.20 g, 0.187 mmol) in ethylene glycol (15 ml), heated to 120°C was added cis-dichlorobis(2,2'-bipyridine)osmium(II) (0.10 g, 0.187 mmol) in 5~10 ml ethylene glycol. The resulted solution was stirred at 140 °C for 48 hours. After cooling down to room temperature, the solution was concentrated to 10 ml and then added into a solution of $(NH_4)PF_6$ (0.25 g) in 80 ml water. A dark solid was collected by filtration and recrystallized from CH_2Cl_2/MeOH to give 0.2 g of product as black shining crystal (57%). ^1H NMR ($CDCl_3$, ppm): d 0.85 (t, J = 6.56 Hz, 12 H, $-CH_3$); 1.20-1.55 (m, 32 H, aliphatic protons); 1.73 (m, 8H, $-CH_2-$); 3.86 (t, J = 5.33 hz, 4H, $-OCH_2-$); 3.97 (t, J = 5.6 Hz, 4H, $-OCH_2-$); 6.90 (d, J = 16.40 Hz, 2 H, vinyl protons); 7.04 (s, 2H, aromatic protons meta to iodo); 7.19 (s, 2H, aromatic protons ortho to iodo); 7.31-7.34 (m, 4H, 2 vinyl protons and 2 ArH); 7.37 (t, J = 6.82 Hz, 2H, ArH); 7.56 (s, 2H, ArH); 7.66-7.70 (m, 8H, ArH); 7.90 (d, J = 8.29 Hz, 2H, ArH); 8.15 (d, J = 8.34 Hz, 2H, ArH); 8.21 (t, J = 5.70 Hz, 4H, ArH);. Anal. Calcd for $C_{74}H_{90}N_6O_4I_2P_2F_{12}Os$: C, 47.74; H, 4.87; N, 4.51. Found: C, 47.67; H, 4.88; N, 4.53.

Compound 12. To a vacuum-dried two neck flask was added 1.89 g of Mg (0.0777 mol) and 30 ml of ether. Octylbromide (15.00 g, 0.0777mol) in 20 ml of ether was then added into the above suspension in such a rate that the reaction mixture maintained self-refluxing. After the addition was completed, the mixture was further refluxed in an oil bath for half an hour. The solution was then transfered into an addition funnel and added dropwise into a mixture containing 1,4-dibromobenzene (19.73 g, 0.0777 mol), $PdCl_2$(dppf) (0.60 g, 0.7 mmol) and 40 ml of ether. The resulted mixture was refluxed overnight and then poured into water. After removal of the catalyst residue (red precipitate) by filtration, the filtrate was extracted with ethyl ether. The organic layer was washed with water, dried ($MgSO_4$) and the solvent was evaporated. The resulted liquid was distilled to give 17 g of product as colorless liquid (76%, b.p: 91-92°C/0.8mmHg). ^1H NMR ($CDCl_3$, ppm): δ 0.87 (t, J = 6.79 Hz, 3H, $-CH_3$), 1.28 (m, 10 H, alkyl protons), 1.56 (m, 2 H, alkyl protons), 2.53 (t, J = 7.31 Hz, 2 H, benzyl protons), 6.89 (d, J = 7.63 Hz, 2H, aromatic protons), 7.32 (d, J = 7.72 Hz, 2 H, aromatic protons).

Compound 13. To a suspension containing Mg (0.90 g, 37.14 mmol), one tiny crystal of iodine and THF (10 ml) was added 1 ml of compound **12** (10.00 g, 37.14 mmol). After stiring for a couple of minutes, the mixture started to reflux. The rest of the compound 12 was then added to the mixture in such a rate as to maintain the refluxing. After the addition was finished, the mixture was refluxed for another half an hour. The resulted greeniard reagent was transferred into an addition funnel and added dropwise into a mixture containing 1,6-dibromohexane (9.06 g, 37.14 mmol), Li_2CuCl_4 (3.71 ml of 0.1M THF solution, 37.14 mmol) and 20 ml of THF at 5-10°C. The resulted mixture was stirred overnight at room temperature and then poured into water. The mixture was extracted with methylene chloride. The organic layer was washed with water, aquaous $NaHCO_3$ solution and water again. It was then dried with $MgSO_4$. After removal of the solvent, the resulted liquid was purified by running through a short filtration column (hexane as the eluent), 9.02 g of pure product was obtained as colorless liquid.(70%) ^1H NMR ($CDCl_3$, ppm): δ 0.87 (t, J = 6.79 Hz, 3 H, $-CH_3$), 1.24-1.34 (m, 12 H, alkyl protons), 1.44 (m, 2 H, alkyl protons), 1.59 (m, 4 H, alkyl protons), 1.83 (m, 2 H, alkyl protons), 2.55 (t, J = 7.20 Hz, 4 H, benzyl protons), 3.36 (t, J = 6.34 Hz, 2 H, $-CH_2Br$), 7.02 (s, 4 H, aromatic protons).

17

Compound 14. A mixture containing compound **13** (9.00 g, 25.47 mmol), iodine (5.19 g, 20.47 mmol), H_5IO_6 (2.332 g, 10.23 mmol), acetic acid(17 ml), 30% sulphuric acid (3 ml) and CCl_4 (8 ml) was stirred at 80 °C for 48 h. It was then poured into aquaous solution of $NaHSO_3$ and extracted with methylene chloride. The organic layer was washed with water, dried ($MgSO_4$) and the solvent was evaporated. The resulted liquid was purified by flash chromatogaphy (hexane as the eluent) to give 11.8 g of product (78%). ^1H NMR ($CDCl_3$, ppm): δ 0.87 (t, J = 6.79Hz, 3H, $-CH_3$), 1.24-1.34 (m, 12H, alkyl protons), 1.46-1.59 (m, 6H, alkyl protons), 1.83 (m, 2H, alkyl protons), 2.55 (t, J = 7.20Hz, 4H, benzyl protons), 3.36 (t, J = 6.34Hz, 2H, $-CH_2Br$), 7.52 (s, 2H, aromatic protons).

Compound 15. A solution of compound **14** (4.00 g, 6.71 mmol), N-methyl aniline (1.078 g, 10.07 mmol), potassiun carbonate (1.85 g, 13.42 mmol), tetrabutylammonium bromide (0.11 g, 0.34 mmol) and sodium iodide (2.02 mg, 0.013 mmol) in toluene (5 ml) was stirred under refluxing overnight. Diethyl ether (25 ml) and water (25 ml) were then added. The organic layer was separated and dried over magnesium sulfate. After removal of the solvent, the residue liquid was purified by chromatography (methylene chloride as eluent) to give 3.1g of product as colorless liquid (73%). ^1H NMR ($CDCl_3$, ppm): δ 0.87 (t, J = 6.79Hz, 3H, $-CH_3$), 1.26-1.37 (m, 14H, alkyl protons), 1.51-1.58 (m, 6H, alkyl protons), 2.56 (t, J = 6.50Hz, 4H, benzyl protons), 2.90 (s, 3H, -NCH_3), 3.28 (t, J = 7.15Hz, 2H, $-CH_2N$), 6.40 (t, J = 7.95 Hz, 3H, aromatic protons), 7.17 (d, J = 7.08Hz, 2H, aromatic protons), 7.52 (s, 2H, aromatic protons).

Compound 16. Phosphorus oxychloride (1.21 g, 7.919 mmol) was added dropwise to DMF (5 ml, 64.6 mmol) at 0 °C. The solution was stirred at 0°C for 1 hour and then at 25°C for another 1 hour. Compound **15** (5.00 g, 7.919 mmol) in 5 ml of DMF was then added dropwise to the mixture. The resulted solution was stirred at 80°C overnight. After being cooled down to room temperature, the solution was poured into cold water and neutralized with NaAc. The mixture was extracted with methylene chloride. The organic layer was washed with water and then dried. After removal of the solvent, hexane was added to the liquid residue. The product crystalized out and collected by filtration as white solid. (3.34 g, 64%, mp: 70-71°C). ^1H NMR ($CDCl_3$, ppm): δ 0.88 (t, J = 6.48 Hz, 3H, $-CH_3$), 1.27-1.64 (m, 20H, alkyl protons), 2.55-2.59 (m, 4H, benzyl protons), 3.02 (s, 3H, -NCH_3), 3.38 (t, J = 7.36Hz, 2H, $-CH_2N$), 6.63 (d, J = 8.61 Hz, 2H, aromatic protons), 7.52 (s, 2H, aromatic protons), 7.66 (d, J = 8.61Hz,2H, aromatic protons), 9.65 (s, 1H, aldehyde proton).

Monomer D. Sodium hydride (0.40 g, 16.51 mmol) was added to a solution of compound **16** (7.26 g, 11.01 mmol) in 1,2-dimethoxyethane (DME) (10 ml). The suspension was stirred for 5 min. and diethyl 4-(methylsulfonyl)benzyl phosphate (3.37 g, 11.01 mmol) in 5 ml of DME was then added dropwise. The resulted solution was stirred at 80°C overnight and then poured into water. The mixture was extracted with methylene chloride. The organic layer was washed with water and dried. After removal of the solvent, the resulted mixture was purified by chromatography (hexane:ethyl acetate=2:1 as eluent) and recrystalization from ether to give 1.8 g of product as greenish yellow solid (50%, mp: 94-95°C). ^1H NMR ($CDCl_3$, ppm): δ 0.87 (t, J = 6.48Hz, 3H, -CH_3), 1.23-1.60 (m, 20H, alkyl protons), 2.57-2.58 (m, 4H, benzyl protons), 2.96 (s, 3H,--SO_2CH_3), 3.03 (s, 3H, -NCH_3), 3.33 (t, J = 6.60Hz, 2H, -CH_2N), 6.62 (d, J = 8.15 Hz, 2 H, aromatic protons), 6.84 (d, J = 16.13 Hz, 1H, vinyl proton), 7.11 (d, J = 16.20 Hz, 1 H, vinyl proton), 7.36 (d, J = 8.39 Hz, 2 H aromatic protons), 7.53-7.55 (m, 4 H, aromatic protons), 7.80 (d, J = 7.97 Hz, 2 H, aromatic protons). Anal. Calcd for $C_{36}H_{47}SNI_2O_2$: C, 53.27; H, 5.84; N, 1.73. Found: C, 53.21; H, 5.86; N, 1.67.

18

Polymerization via the Heck coupling reaction. A typical polymerization was exemplified by the synthesis of polymer **2**: Triethylamine (0.19ml, 1.36mmol) was added to a solution of monomer **A** (0.0458 g, 0.0258 mmol), Monomer **B** (0.4000 g, 0.517 mmol), p-divinylbenzene (0.0707 g, 0.543 mmol), $Pd(OAc)_2$ (4.9 mg,0.0217 mmol), and tri-0-tolylphospine (32.9 mg, 0.108 mmol) in 5-10 ml DMF. The resulting mixture was stirred at 80 °C overnight under a nitrogen atmosphere and was then poured into methanol. The precipitated polymer was collected by filtration, redissolved in tetrchloroethane and reprecipitated into methanol. The polymer was further purified by extraction in a Soxhlet extractor with methanol for 24 h and dried under a vacuum at 50 °C for 2 days.

Polymer 1. ^1H NMR ($CDCl_2$-$CDCl_2$, ppm): δ 0.88 (broad, 3H, -CH_3 in alkoxyl chain), 1.21 (b, 3H, -CH_3 in chromophore), 1.38, 1.49, 1.71, 1.80 (4 broad peaks, each has 2H, methylene protons), 2.87 (m, 3H, -SO_2Me), 3.48 (b, 2H, -NCH_2CH_3) 3.79 (b, 2H, -NCH_2CH_2O-), 4.00 (b, 2H, -OCH_2- in alkoxyl chain), 4.20 (b, 2H, -OCH_2CH_2N-), 6.75 (b, 4H, aromatic protons), 7.02 (b, 5H, vinyl protons), 7.38 (b, 5H, 4 aromatic and 1 vinyl protons), 7.46 (b, 4H, aromatic protons), 7.69 (m, 2H, aromatic protons). Anal. Calcd. for $C_{41}H_{45}NO_4S$: C, 76.04; H, 6.96; S 4.94. Found: C, 74.38; H, 7.00; S, 5.09

Polymer 2. ^1H NMR spectra of polymer 2 is very similar to that of polymer 1 except some small peaks due to the ruthenium complex (8.00, 8.5ppm). Anal. Calcd. for $C_{43.15}H_{47.65}N_{1.25}O_4S_{0.95}P_{0.1}F_{0.6}Ru_{0.05}$: C, 74.28; H, 6.83; N, 2.49; Ru, 0.69. Found: C, 73.36; H, 6.98; N, 2.67; Ru, 0.55.

Polymer 3. ^1H NMR spectra of polymer 5 is very similar to that of polymer 3 except some small peaks due to the osmium complex (4.0, 8.00, 8.5 ppm). Anal. Calcd. for $C_{47.9}H_{57.15}N_{1.25}O_{2.1}S_{0.95}P_{0.1}F_{0.6}Os_{0.05}$: C, 74.02; H, 6.98; N, 2.38. Found: C, 71.48; H, 6.73; N, 2.36.

Polymer 4. ^1H NMR ($CDCl_3$, ppm): δ 0.87 (broad, 3H, -CH_3 in alkyl chain), 1.19-1.16 (b, 20H,aliphatic protons), 2.74 (b, 4H, benzyl protons), 2.92 (b, 3H, -SO_2Me), 2.99 (b, 3H, -NCH_3), 3.31 (b, 2H, -NCH_2-), 6.59 (b, 2H, aromatic protons), 6.99 (m, 1H, vinyl protons), 7.02 (b, 2H, aromatic protons), 7.07 (d, J = 16.85 Hz, 1H, vinyl proton), 7.32 (b, 2H, aromatic protons), 7.40 (b, 4H, vinyl protons), 7.49 (b, 6H, aromatic protons), 7.77 (m, 2H, aromatic protons). Anal. Calcd. for $C_{46}H_{55}SNO_2$: C, 80.54; H, 8.08; N, 2.04. Found: C, 80.50; H, 8.02; N, 2.08.

Polymer 5. ^1H NMR spectra of polymer 5 is very similar to that of polymer 4 except some small peaks due to the ruthenium complex (4.0, 8.00, 8.5 ppm). Anal. Calcd. for $C_{47.9}H_{57.15}N_{1.25}O_{2.1}S_{0.95}P_{0.1}F_{0.6}Ru_{0.05}$: C, 78.38; H, 7.85; N, 2.38, Ru, 0.67 Found: C, 76.48; H, 7.72; N, 2.41, Ru, 0.50

Compound 21. Compound **21** was synthesized from compound **5** (see chapter four) by a similar approach as the synthesis of compound **6** (2 eq. of butyl lithium was used). mp. 74-75°C. ^1H NMR ($CDCl_3$, ppm): 0.90 (t, J = 6.50 Hz, 6H, -CH_3), 1.33 (m, 8H, methylene protons), 1.46 (m, 4H, methylene protons), 1.79-1.84 (m, 4H, methylene protons), 4.05 (t, J = 6.16 Hz, 4h, -OCH_2-), 7.37 (s, 2H, aromatic protons), 10.44 (s, 2H, aldehyde protons). Anal. Calcd for $C_{20}H_{30}O_4$: C, 71.82; H, 9.04; O, 19.14. Found: C, 71.69; H, 9.11.

Compound 22. The mixture of α,α'-dibromo-p-xylene (4.73 g, 17.99 mmol) and $P(OEt)_3$ (8.97 g, 53.98 mmol) was stirred at 120 °C for 4 hours. The excess amount of $P(OEt)_3$ was distilled out. The residual liquid solidified to give the product as a white solid. (6.10 g, 90%, mp.

73-74°C). ^1H NMR (CDCl$_3$, ppm): 1.23 (t, J = 6.80 Hz, 12H, -CH$_3$), 3.10 (d, J = 20.51Hz, 4H, benzyl protons), 3.96-3.99 (m, 8H, -OCH$_2$-), 7.19 (s, 4H, aromatic protons). Anal. Calcd for C$_{16}$H$_{28}$O$_6$P$_2$: C, 50.79; H, 7.46; O, 25.37. Found: C, 50.69; H, 7.44.

Compound 23. A mixture of compound **6** (0.60 g, 1.388 mmol), vinyl tributyltin (0.44 g, 1.388 mmol) and Pd(PPh$_3$)$_4$ (0.032 g, 0.0278 mmol) in DMF (8 ml) was stirred at 100 °C for four hours. After cooling down to room temperature, the mixture was filtered and the filtrate was poured into water. After extraction with ethyl ether, the organic layer was collected and dried over MgSO$_4$. After removal of the solvent, the crude product was purified by chromatography (hexane:ethyl acetate = 20:1 as eluent) to give the product. (0.24 g, 52%, mp. ??) ^1H NMR (CDCl$_3$, ppm): 0.86-0.93 (m, 6H, -CH$_3$), 1.26-1.46 (m, 12H, methylene protons), 1.75-1.83 (m, 4H, methylene protons), 3.95 (t, J = 6.51 Hz, 2H -OCH$_2$-), 4.04 (t, J = 6.38 Hz, 2H, -OCH$_2$-), 5.38 (d, J = 11.30Hz, 1H, vinyl proton), 5.80 (d, J = 17.71Hz, 1H, vinyl proton), 7.01 (m, 2H, 1 vinyl and 1 aromatic protons), 7.24 (s, 1H, aromatic proton), 10.36 (s, 1H, -CHO).

Monomer E. The typical Heck reaction condition as for polymerization was applied. Product was purified by chromatography (H:EA=10:1 as eluent) and recrystalized from methylene chloride/methanol. Yield: 38%, mp. 123-124°C. ^1H NMR (CDCl$_3$, ppm): δ 0.87-0.91 (m, 15H, -CH$_3$ in alkoxy); 1.23 (t, J = 7.08 Hz, 3 H, -CH$_3$ on chromophore), 1.27-1.38 (m, 22H, aliphatic protons), 1.47-1.55 (m, 10H, aliphatic protons), 1.80-1.87 (m, 10H, aliphatic protons), 3.04 (s, 3H, -SO$_2$CH$_3$), 3.51 (t, J = 7.04Hz, 2H, N-CH$_2$-CH$_3$), 3.81 (t, J = 5.60 Hz, 2H, -CH$_2$-CH$_2$-N), 3.97-4.08 (m, 10H, -OCH$_2$- on alkoxy side chain), 4.22 (t, J = 5.81 Hz, 2H, -OCH$_2$-CH$_2$N-), 6.70 (d, J = 8.57 Hz, 2H, aromatic protons), 6.74 (d, J = 16.39 Hz, 1H, vinyl proton), 7.02 (d, J = 16.23, 1H, vinyl proton), 7.08 (d, J = 6.56Hz, 2H, aromatic protons), 7.10 (d, J = 15.50Hz, 2H, vinyl protons), 7.25 (s, 1H, aromatic proton), 7.28 (s, 2H, aromatic protons), 7.30 (s, 1H, aromatic proton), 7.39 (d, J = 16.45Hz, 1H, vinyl proton), 7.44 (s, 1H, aromatic proton), 7.46 (s, 1H, aromatic proton), 7.49 (d, J = 8.06 Hz, 2H, aromatic protons), 7.52 (d, J = 16.56 Hz, 1H, vinyl proton), 7.80 (d, J = 8.15 Hz, 2H, aromatic protons), 10.33 and 10.34 (s, 2H, -CHO). Anal. Calcd. for C$_{74}$H$_{101}$NO$_{10}$S: C, 74.27; H, 8.51; N, 1.17. Found: C, 74.29; H, 8.47; N, 1.21.

Model reaction. The reaction condition was similar to the above. The reaction mixture was poured into 5% hydrochloric acid solution, extracted with ethyl ether. The organic layer was washed with water, dried over MgSO$_4$ and then the solvent was removed. After collecting the ^1H NMR, the residue was separated by chromatography (hexane:ethyl acetate = 6:1 as the eluent) to give compounds **18,19,** and **20**. The relative yield was calculated based on the ^1H NMR spectrum. The characterizations of the products were exemplified by entry a (2,5-dihexoxyl-1,4-diiodo benzene as the reactant) as below:

Compound 18. Purified yield, 78%. ^1H NMR (CDCl$_3$, ppm): 0.92 (t, J = 6.58 Hz, 6H, -CH$_3$), 1.37 (m, 8H, methylene protons), 1.53 (m, 4H, methylene protons), 1.85 (m, 4H, methylene protons), 4.02 (t, J = 6.21 Hz, 4H, -OCH$_2$-), 7.07 (s, 2H, aromatic protons), 7.08 (d, J = 15.98, 2H, vinyl protons), 7.30 (t, J = 7.40, 6H, aromatic protons), 7.42 (d, J = 16.51, 2H, vinyl protons), 7.47 (d, J = 7.38, 4H, aromatic protons). ^{13}C NMR (CDCl$_3$, ppm): 14.0, 22.6, 25.9, 29.4, 31.6, 69.4, 110.5, 123.4, 126.4, 126.7, 127.3, 128.6, 137.9, 151.0. Anal. Calcs. for C$_{34}$H$_{42}$O$_2$: C, 84.60; H, 8.77. Found: C, 84.72; H, 8.76.

Compound 19. Purified Yield, 11.7% . ^1H NMR (CDCl$_3$, ppm): 0.82 (m, 3H, -CH$_3$), 0.92 (m, 3H, -CH$_3$), 1.02 (m, 2H, methylene protons), 1.10 (m, 2H, methylene protons), 1.18 (m, 2H,

methylene protons), 1.33 (m, 6H, methylene protons), 1.52 (m, 2H, methylene protons), 1.81 (m, 2H, methylene protons), 3.73 (t, J = 6.11 Hz, 2H, -OCH$_2$-), 3.96 (t, J = 6.03 Hz, 2H, -OCH$_2$-), 5.30 (s, 1H, vinyl proton), 5.60 (s, 1H, vinyl proton), 6.81 (s, 1H, aromatic proton), 7.04 (s, 1H, aromatic proton), 7.07 (d, J = 16.30, 1H, vinyl proton), 7.18-7.31 (m, 8H, aromatic protons), 7.42-7.48 (m, 3H, 2 aromatic protons + 1 vinyl proton). ^{13}C NMR (CDCl$_3$, ppm): δ, 13.99, 22.41, 22.58, 25.29, 25.88, 29.06, 29.39, 31.48, 31.56, 68.96, 69.35, 110.49, 115.27, 115.97, 123.47, 126.40, 126.56, 126.74, 127.16, 127.26, 127.88, 128.51, 128.66, 131.57, 137.88, 141.47, 147.52, 150.63, 150.72. Mass spectra m$^+$/e = 482.3 (required 482.32).

Polymerization via the HWE reaction. Typical polymerization procedure was exemplified by the synthesis of polymer **8**: Monomer **E** (0.5680 g, 0.475 mmol) was dissolved in THF (5 ml) and NaH (0.0340 g, 1.42 mmol) was then added. A solution of compound **22** (0.1710 g, 0.451 mmol) and compound **3** (0.0110 g, 0.024 mmol) in THF (5 ml) was added into the above solution while stirring. The resulted mixture was refluxed for 4 hours and the red polymer started to precipitate out. The reaction was stopped and the mixture was poured into methanol. The polymer was collected by filtration and purified by extraction in a Soxhlet extractor with methanol for 24 h. It was then dried under a vacuum at 50 °C for 2 days (0.55 g, 91%).

Polymer 7. ^{1}H NMR (CDCl$_2$-CDCl$_2$, ppm): d 0.90 (b, 6H, -CH$_3$), 1.35 (b, 8H, -(CH$_2$)$_2$-), 1.50 (b, 4H, -CH$_2$-), 1.85 (b, 4H, -CH$_2$-), 4.05 (b, 4H, -OCH$_2$-), 7.10 (b, 4H, vinyl protons), 7.48 (b, 6H, aromatic protons). Anal. Calcs. for C$_{28}$H$_{36}$O$_2$: C, 83.17; H, 8.91. Anal. Calcd. for C$_{28}$H$_{36}$O$_2$: C, 83.17; H, 8.91. Found: C, 81.58; H, 8.84.

Polymer 8. Similar ^{1}H NMR spectrum as polymer **9** was obtained. Since the solubility of polymer **9** is much better than polymer **8** in CDCl$_3$, ^{1}H NMR data of polymer 11 was presented here.

Polymer 9. ^{1}H NMR (CDCl$_3$, ppm): δ 0.89 (b, 15H, -CH$_3$ in alkoxy); 1.25 (b 3H, -CH$_3$ on chromophore), 1.35 (m, 22H, methylene protons), 1.55 (b, 10H, methylene protons), 1.87(m, 10H, methylene protons), 3.04 (b, 3H, -SO$_2$CH$_3$), 3.55 (b, 2H, N-CH$_2$-CH$_3$), 3.80 (b, 2H, -CH$_2$-CH$_2$-N), 4.10 (b, 10H, -OCH$_2$- on alkoxy side chain), 4.22 (b, 2H, -OCH$_2$-CH$_2$N-), 5 broad peaks at 6.70, 7.15, 7.31, 7.48, 7.70 were observed which couldn't unambiguously assigned. Anal. Calcd for : C, 74.02; H, 6.89; Ru, 0.72. Found: C, 75.33; H, 8.24; Ru, 0.09.

Characterization. The ^{1}HNMR spectra were collected on a Varian 500-MHz FT NMR spectrometer. The FTIR spectra were recorded on a Nicole 20 SXB FTIR spectrometer. A Shimadzu UV-2401PC UV/vis spectrometer was used to record the UV/vis spectra. Thermal analyses were performed by using the DSC-10 and TGA-50 systems from TA Instruments under a nitrogen atmosphere. The melting points were obtained with open capillary tubes on a Mel-Tem apparatus without corrections. Elemental analyses were performed by Atlantic Microlab, Inc., except the ruthenium analyses, which were done by Galbraith Laboratories, Inc.. Molecular weights were measured with a Waters RI GPC system using polystyrene as the standards and THF as the eluent.

The photoconductivity was studied by measuring the voltage across a 1 MΩ resistor resulting from a photocurrent running through the sample. A Diode laser (690 nm) with an intensity of 20 mW was used as the light source.[24]

Second-order NLO properties of poled polymeric films were characterized by second harmonic generation measurements. A mode-lock Nd:YAG laser (Continuum-PY 61 C-10, 10-Hz repetition rate) was used as the light source. The second harmonic of the fundamental wave (1064

21

nm) generated by the polymer sample was detected by a photomultiplier tube (PMT), then amplified and averaged in a boxcar integrator. To measure the temperature dependence of the second order nonlinearity, a polymer film was mounted to a heating stage. The transmitted SHG signal was monitored while the sample was heated up.

The linear electrooptic coefficient , r_{33}, of the poled polymer films was measured at 690 nm using a reflection method.[14] A Soleil-Babinet compensator was used to bias the DC intensity at its half maximum intensity. The phase retardation between the p and s waves was modulated by an external oscillating field. The modulation of the intensity amplitude was determined using a lock-in amplifier, which was then used to calculate the r_{33} value.

A two-beam coupling experiment was performed using a diode laser (690 nm, 25 mW, Laser Power Technology, 690-300) as the laser source. The laser beam (s-polarized) was split into two beams, which were intersected in the polymer film at a geometry reported before.[25] The transmitted intensities of the two beams were monitored by Lock-in amplifiers and collected by a computer.

To measure the phase shift of the refractive index grating over the intensiy interference pattern, a motor driven pizoelectric translator was used to move the sample along the grating vector. The transmitted intensity of the two beams were collected in the same way as the two beam coupling experiment.

The photorefractive (PR) effect involves a photoinduced change of the refractive index in an optically nonlinear and photoconducting material.[1] This effect arises when photogenerated charge carriers separated by drift and/or diffusion processes and become trapped to produce a nonuniform charge density distribution. This charge separation creates an internal space-charge field which modulates the refractive index of the material through the electro-optic effect. The refractive index grating can be formed in experiments such as two-beam coupling and four-wave mixing, and be detected by utilizing these holographic techniques.

## B. A Multifunctional Photorefractive Molecule Showing High Optical Gain and Diffraction Efficiency

A convenient approach to prepare PR polymers is to mix all the necessary molecular components into a polymer matrix forming a composite.[5-7] Extremely large photorefractive effects were observed in some systems when specific compositions were used.[8-12] A general observation is that only those composite materials which have low glass transition temperatures (lower than room temperature) show large net optical gain. It was suggested that the chromophore reorientation in response to the photoinduced internal field greatly enhanced the photorefractive performance in these materials.[13] However, one major drawback for these composite materials is their phase separation, caused by the incompatibility between small molecules and the polymer host. In some cases, the phase separation may completely ruin their optical properties.

To utilize the advantage of the orientational enhancement, and at the same time to minimize the phase separation, we designed and synthesized a simple, small molecular system which contains a 3-alkyl-substituted oligothiophene molecule covalently connected to a nonlinear optical (NLO) chromophore. The design concept of this molecule is inherited from our previous work on conjugated photorefractive polymers.[14] The molecule contains all the functionalities necessary to show the PR effect. The oligothiophene is photoconductive in the visible light region. The E-O component could be generated by aligning the dipoles of the NLO chromophore under an applied electric field. Another interesting point is that amorphous films can be prepared by sandwiching

them between two indium tin oxide (ITO) glass slides. The films thus made can be maintained in amorphous state for a long time.

The synthesis of the photorefractive compound is shown in Scheme 1. In our previous publication,[16] we have described the synthesis of oligothiophene aldehyde **3**. The Wittig reaction between aldehyde **3** and phosphonate **2** in refluxing ethylene glycol dimethyl ether, followed by the hydrolysis in a base condition, afforded the carboxylate acid **4**. The target molecule (compound **6**) was synthesized in 75% yield by utilizing the Mitsunobu reaction between compound **4** and the NLO chromophore **5**. Compound **6** is a red solid at room temperature and is quite soluble in most of the organic solvents.

Scheme 9. Synthesis of oligothiophene containing photorefractive material:
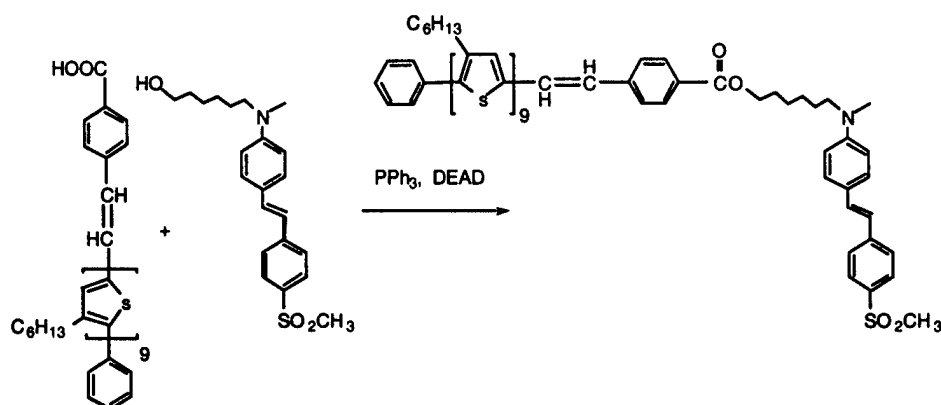
The structure of compound **6** was confirmed by ^{1}H NMR, ^{13}C NMR and elemental analysis. The UV/vis spectrum of compound **6** in CHCl$_3$ shows a red shift of 24 nm in the absorption peak compared with the absorption spectrum of the NLO chromophore **5**. The solid-state UV/vis spectrum of compound **6** exhibits the absorption maximum at 440 nm and a tail extending beyond 600 nm (Figure 4). This red-shifted absorption enables us to excite the compound by utilizing a He-Ne laser (λ = 632.8 nm).
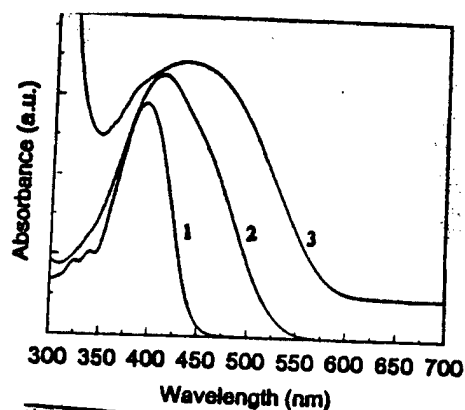

Figure 4. UV/vis spectra of the NLO compound **5** in CHCl$_3$(1), compound **6** in CHCl$_3$(2) and solid-state(3).

To prepare films for physical studies, a filtered solution of compound **6** in CH_2Cl_2 was cast manually onto ITO glass substrates and dried under vacuum overnight to remove the solvents. The films were then slightly heated to further soft the material and sandwiched with another ITO glass substrate. A typical film thickness ranged from 60 μm to 75 μm.

The films prepared from the CH_2Cl_2 solution are transparent and photoconductive as studied at the working laser wavelength of 632.8 nm. The photoconductivity was determined at 632 nm by measuring the voltage which resulted from the passing of the photocurrent through the thin film and a 1-MΩ resistor. A lock-in amplifier was used to measure the photovoltage. A photoconductivity of ca. 1.59×10^{-9} $\Omega^{-1}cm^{-1}/(W/cm^2)$ was obtained for compound **6** under an external electric field of 462 KV/cm. The photocurrent was found to be electric field-dependent as shown in Figure 5; as the electric field increases, the photocurrent increases, a phenomenon similar to most of the PR polymers. The dark conductivity of this sample also increases with the applied electric field but remains at least one magnitude lower than the photoconductivity. From the photocurrent results, the maximum quantum yield was estimated to be 1.05×10^{-2} at an applied field of 462 kv/cm.

The external elextric field was applied across the films sandwiched between two ITO coated glass substrates so that the dipole of the NLO chromophore can be aligned. To confirm the electro-optic response of the films, second harmonic signal as a function of the electric field at room temperature were performed by using a fundamental frequency (1064 nm) of a model-locked Nd:YAG laser. The second harmonic coefficient, d_{33}, shows a trend of leveling off as the field further increases, possibly due to the saturation of the electric field induced chromophore alignment (Figure 5b).
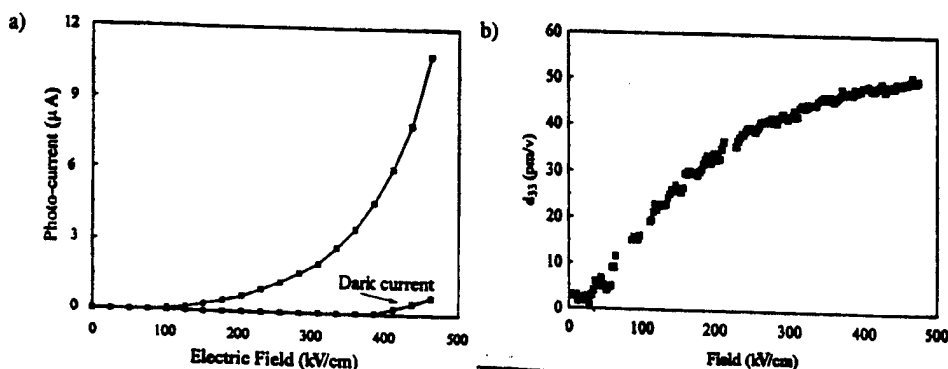

Figure 5. a). The photocurrent and dark current response of compound **6** as a function of the external electric field. b). The second harmonic generation coefficient d_{33} of compound **6** as a function of the external electric field.

The photorefractive properties of our material were examined by the two-beam coupling, four-wave mixing, and holographic image formation experiments at different applied electric fields. In the two-beam coupling experiment, two coherent laser beams (632.8 nm, 30 mw, *p*-polarized) intersect upon the PR sample to generate the refractive index grating. The grating which has a nonzero phase shift with the light intensity pattern leads to the asymmetric energy exchange between the two beams, characterized by the two beam coupling gain coefficient, Γ. The two writing beams have comparable intensities. The normal of the sample was tilted by 30° with respect to the bisector of the two writing beams in order to obtain a non-zero projection of the E-O coefficient. The

experiment was carried out by chopping one of the two incident beams while monitoring the transmitted intensity of the other. The gain coefficient Γ could be calculated from the intensities of the two beams by the following equation:[1]

$$\Gamma = \frac{1}{L} \ln(\frac{1 + \alpha}{1 - \beta\alpha})$$

where L is the optical path length for the beam with gain, α is the ratio of the intensity modulation of the signal beam $\bullet I_s/I_s$, and β is the intensity ratio of the two writing beams I_s/I_q.
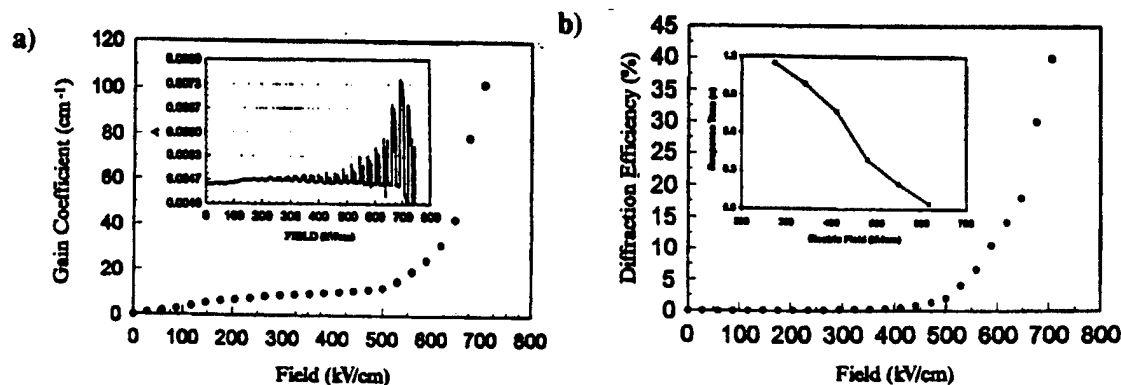

Figure 6. a). The dependence of the two-beam coupling gain coefficient on the applied external electric field. The inset shows the two-beam coupling signal at a fixed electric field. b). The dependence of the diffraction efficiency on the applied external electric field. The inset shows the field dependence of the response time.

After the electric field was switched on, the asymmetric energy transfer between the two beams was observed (inset of Figure 6). The gain coefficient Γ also showed a strong dependence on the applied electric field (Figure 6). This strong field dependence of the optical gain was anticipated because of the fact that both the SHG signal and the quantum yield of the photogeneration of charge carriers are strongly dependent on the external field. A Γ value of 102 cm^{-1} was obtained at E = 706 kv/cm, which exceeds the absorption coefficient (19 cm^{-1} at 632.8 nm) in this sample, giving a net optical gain of 83 cm^{-1}. When the field was switched off, the gain and loss signals disappeared immediately, eliminating the possibility of beam coupling due to thermal grating.[11]

The index grating formed can be probed by the four wave mixing (FWM) experiment where the diffraction efficiency of a probe laser beam (λ = 780 nm, 3 mw, p-polarized) from the photorefractive grating was measured. The probe beam was diffracted by the index grating according to the Bragg diffraction condition. The diffraction efficiency η is calculated as the intensity ratio of the diffracted light and the probe light. As shown in Figure 6, the diffraction efficiency also has a strong dependence on the electric field and reaches almost 40% at E = 706 kv/cm. From this value, a refractive index modulation of $\bullet n = 2.55 \times 10^{-3}$ was estimated according to the following expression:[12]

$$\eta = \sin^2[\frac{\pi d\Delta n \cos(\theta_1 - \theta_2)}{\lambda\sqrt{\cos\theta_1 \cos\theta_2}}]$$

where d is the sample thickness, λ is the probe laser wavelength, and θ_1 and θ_2 are the internal angles of incidence of the two writing beams.

25

A very interesting feature is that this materials exhibits a fast response to optical signal. A response time of 42 ms was obtained at an applied field of 616 kv/cm in FWM experiments. The response time was extracted from the initial growth of the diffracted signal by fitting with the function $\eta(t)\sim\exp[-2t/\tau]$ for the single-carrier model of refractive grating kinetics.[9, 17] The response time was also found to be field dependent: as the electric field increased, the response time decreased (inset of Figure 6). This is one of the fastest response time reported in organic PR materials.

By inserting a mask into one of the writing beams in the FWM experiment, a photorefractive hologram can be written in the sample. The image was carried onto the sample by an expanded beam and then was focused on the sample. The hologram can be read by the probe beam under the Bragg condition as the diffracted signal and was recorded by a CCD camera. Figure 7 shows a series of holograms recorded under various electric field. Erasure of the holograms occurred quickly upon blocking one of the writing beams.
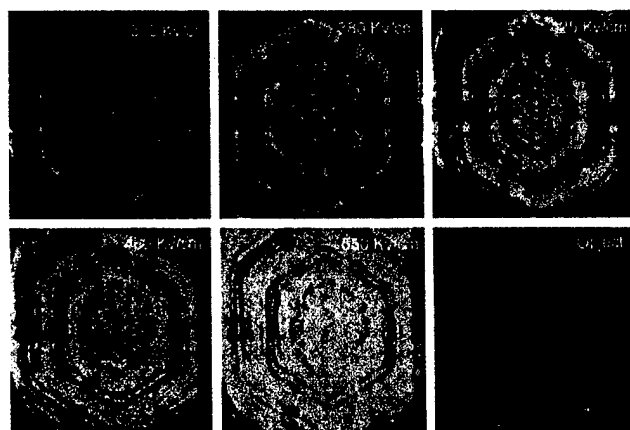

Figure 7. Holographic image formation at different applied field. The object is shown in the bottom right of the series.

These results indicate that a multifunctional small molecule can exhibit high photorefractive performance if the molecule is carefully designed. This pointed to a new direction for the development of photorefractive organic materials. Comparing to polymer systems, mutifunctional molecular system shows advantage in defining the molecular structure and in purification of the material. The sample preparation become easier than corresponding polymer systems. The fast respnse time observed in this system is also a very usefyl bonus for its application in signal processing.

In conclusion, a single PR molecule was designed and synthesized by combining a oligothiophene segment with a nonlinear optical (NLO) chromophore. The conjugated oligothiophene moisty played the roles of the photocharge generator and the charge transporter. The PR properties of this molecule showed a strong dependence on the applied electric field due to the orientational enhancement effect as well as the linear electrooptic effect. Large net optical gain coefficient and diffraction efficiency, as well as a fast response time, were achieved in this small molecule system.

Synthesis of the compound: Diethyl azodicarboxylate (DEAD) (40 mg, 0.23 mmol) was added to a solution of compound **A** (280 mg, 0.16 mmol), compound **B** (81 mg, 0.21 mmol) and

triphenylphosphine (60 mg, 0.23 mmol) in 3 ml THF. The mixture was stirred at room temperature for 3 h. After the solvent was removed with a rotary evaporator, the crude product was purified by a silica gel chromatography column using hexane / ethyl acetate (2 / 1) as the eluent to give the compound as a red amorphous solid (0.25 g, 75% yield). ^{1}H NMR (CDCl$_3$, ppm) δ 8.01 (d, 2 H), 7.86 (d, 2 H), 7.60 (d, 2 H), 7.50 (d, 2 H), 7.42 (m, 6 H), 7.36 (m, 1 H), 7.24 (d, 1 H), 7.18 (d, 1 H), 7.03 (s, 1 H), 6.98 (m, 8 H), 6.89 (d, 1 H), 6.88 (d, 1 H), 6.68 (d, 2 H), 4.32 (t, 2 H), 3.37 (t, 2 H), 3.04 (s, 3 H), 2.99 (s, 3 H), 2.80 (t, 16 H) 2.67 (t, 2 H), 1.68 (m, 20 H), 1.34 (m, 60 H), 0.91 (m, 24 H). Anal. Calcd for C$_{127}$H$_{165}$NS$_{10}$O$_4$: C, 72.97; H, 7.96. Found: C, 73.05; H, 7.99.

C. Synthesis and Unusual Physical Behavior of A Photorefractive Polymer Containing Tri(bispyridyl) Ruthenium(II) Complexes as Photosensitizer and Exhibiting a Low Glass-Transition Temperature
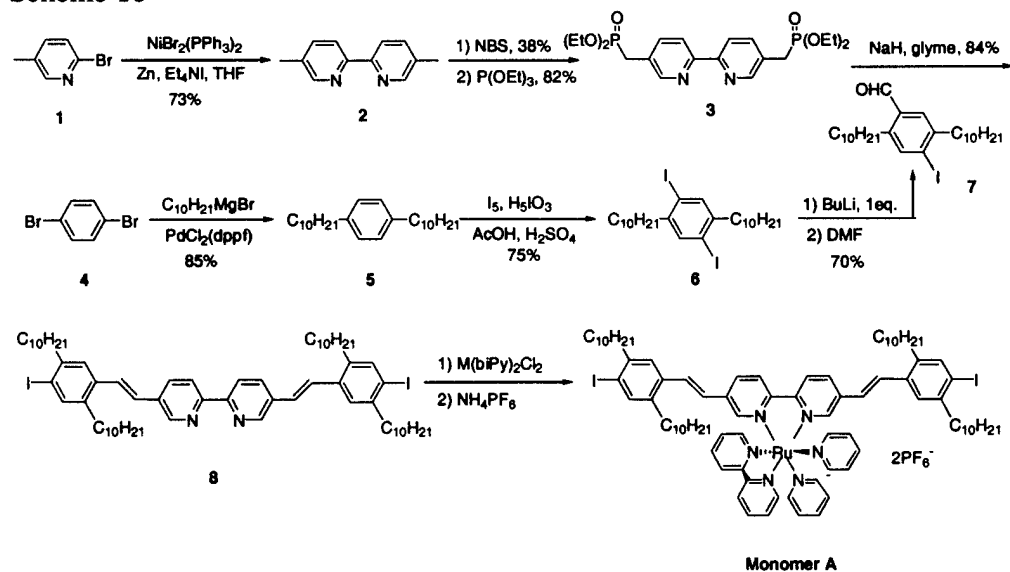
A popular approach to the preparation of PR polymers is to mix all the necessary functional species into polymer matrices, forming composites.[5] For example, large photorefractivity has been achieved in PR composite based on poly(N-vinylcarbazole) (PVK) polymers. Some of the characteristic parameters have matched or even exceeded those of their inorganic counterparts, for example, a nearly 100% diffraction efficiency and 200 cm^{-1} net optical gain have been obtained.[6] A general observation in the composite PR polymeric materials is that only those systems with low glass transition temperatures (T$_g$) (below or slightly above room temperature) give rise to large net optical gain. This phenomena is referred to as the "orientational enhancement effect",[7] in which NLO chromophores can be reoriented under the influence of the space charge field at ambient temperature. This effect leads to a spatial modulation of the birefringence coming from both the optical anisotropy of chromophore and electrooptic (E-O) effect, which greatly improves the magnitude of the refractive index grating. In fact, for the low T$_g$ PR materials the orientational effect makes a greater contribution to the photorefractive gain than does the linear E-O effect.[8]

However, our work mainly focuses on the synthesis and characterizations of fully functionalized materials, in which all functional species are covalently attached to a polymer backbone. Compared with composite PR polymers, fully functionalized PR polymers enjoy the advantage of long-term stability and minimized phase separation. Several systems have been successfully explored, such as functionalized polyurethanes,[9] functionalized conjugated polymers[10] and polyimides containing porphyrin and NLO chromophore units.[11] More recently, we developed a new PR polymer system, i.e., a hybridized PR polymer that contains an ionic tri(bispyridyl) ruthenium complex as the charge generating species, a conjugated polymer backbone as the charge transporting channel and an NLO chromophore.[12-13] The ruthenium complex was introduced to utilize its efficient photoinduced metal-to-ligand charge transfer (MLCT) process so that problems of low quantum yield for the photogeneration of charge carriers in organic materials can be addressed. This PR polymer system has displayed greatly enhanced PR performance; a net optical gain of about 200 cm^{-1} was obtained. That is one of the largest net optical gains reported so far. This PR response, however, is mainly due to the linear E-O contribution because the polymer exhibits a high glass transition temperature (130 ^{0}C) and the dipoles of the NLO chromophores can not be reoriented in responding to the periodical space-charge field. We reasoned that if the Tg of the polymer was lowered without making large change in the polymer structure, we may have the chance to further enhance the PR performance by combining a highly efficient photocharge generator, an efficient charge transportor, the large E-O contribution and the orientational
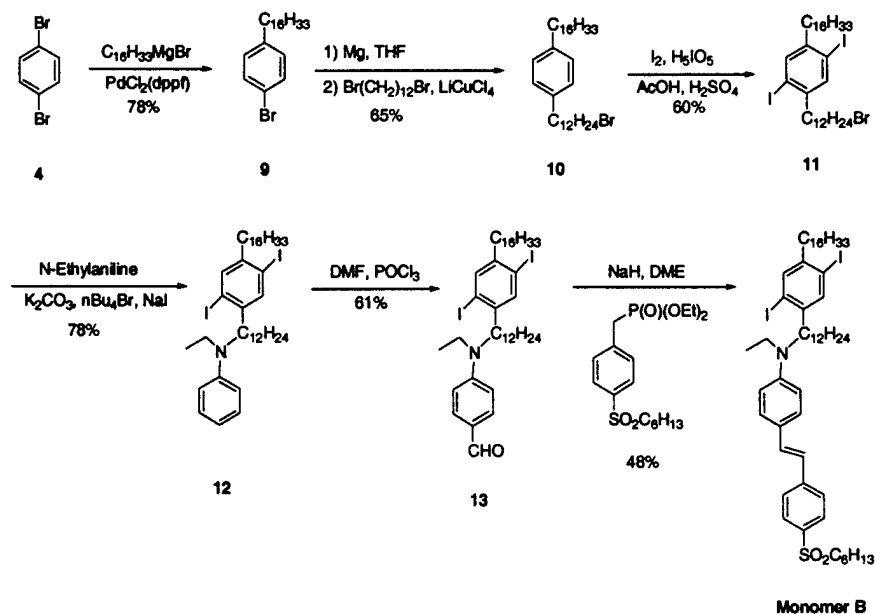
enhancement associated with low T_g materials. We succeeded in synthesizing such a polymer containing transition metal complexes and a conjugated system and exhibiting a T_g of 11 $^{\circ}$C. However, detailed physical studies revealed an interesting phenomenon: at high external electric field, the PR efficiency of this polymer was hindered by the local internal field which is induced by

ion dipole moment formed between the Ru(II) complex and its counterion $(PF_6)^-$. To our knowledge, this is the first time that such a local field effect on the photocharge generation and the PR response was observed. This kind of local field effect on the photocharge generation efficiency may also be a general issue in other field. Any electric field assist charge separation processes, such as those in solar cells, xerographic layer, may be subject to such an effect. In this paper we report the synthesis and physical characterization of a low T_g conjugated polymer containing Ru(II)-tri(bispyridiyl) complexes and pendant NLO chromophores.

    Synthesis and Structural Characterization: The syntheses of monomers are outlined in the Schemes 10 and 11. 5,5'-Dimethyl 2,2'-bipyridine (**2**) was prepared by homocoupling of 2-bromo-5-picoline (**1**) using a nickel catalyst which was generated in situ by reduction of $NiBr_2(PPh_3)_2$ with zinc in the presence of Et_4NI. This approach is advantageous over the method catalyzed by the Raney nickel because its reaction condition is mild and reaction yield is normally better than the later one.[14] In stead of using alkoxy side chains, long alkyl side chains were introduced into monomers. These side chains help to increase the solubility and processibility of the resulting conjugated polymers and to lower the T_g of polymers. Another advantage of introducing alkyl chain is that the absorption the poly(p-phenylenevinylene) (PPV) backbone of the resulting polymer is blue shifted compared to those with alkoxy substitutes. This blue shift minimize the absorption overlap between the π-π^* transition of PPV backbone and the MLCT transition of the Ru complex.[13] Thus, charge carriers can be selectively generated from the Ru complexes center by using longer wavelength laser (He-Ne, 632.8 nm).
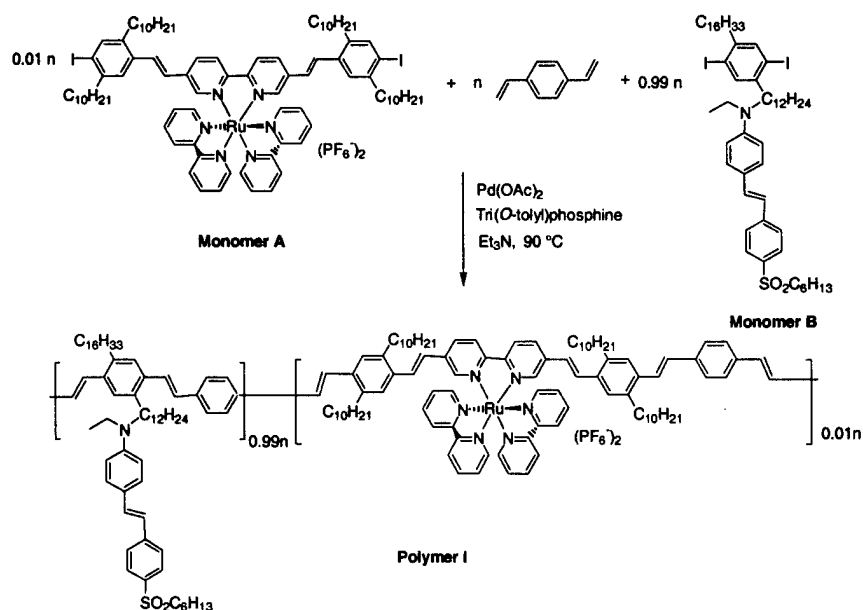
Scheme 10

Monomer A

Scheme 11

4 → **9** → **10** → **11**

C16H33MgBr / PdCl2(dppf), 78%

1) Mg, THF 2) Br(CH2)12Br, LiCuCl4, 65%

I2, H5IO5 / AcOH, H2SO4, 60%

N-Ethylaniline / K2CO3, nBu4Br, NaI, 78% → **12**

DMF, POCl3, 61% → **13**

NaH, DME / P(O)(OEt)2 / SO2C6H13, 48% → **Monomer B**

Scheme 12

Monomer A + n (divinylbenzene) + 0.99 n **Monomer B**

Pd(OAc)2
Tri(O-tolyl)phosphine
Et3N, 90 °C

Polymer I

The polymerization was carried out according to Scheme 12, using a catalytic system composed of Pd(OAc)2/P(o-tolyl)3/n-Bu3N (4%/20%/250%, mole percentage *vs* monomers). The resulting polymer, is soluble in most common organic solvents, such as THF, chloroform, DMF, etc. GPC measurements in THF, using polystyrene as standard, indicated a number-average molecular weight (Mn) of approximately 18 kdalton with a polydispersity (PD) of ca. 1.9.

The structural characteristics of polymers were provided by ¹H NMR, UV/vis spectroscopy and elemental analysis. Since the resulting polymers contain only 1% of the Ru complexes, the ¹H

29

NMR spectrum of the polymer is dominated by the chemical shift of the chromophore and the PPV backbone. However, chemical shifts due to the bipyridyl ligand protons (8.0, 8.4 ppm) still can be observed, indicating the incorporation of the ruthenium complex into the polymer. Some small peaks at 5.2 and 5.8 ppm, which are believed to be introduced by side reactions of the Heck reaction,[15] were also found (about 1-2%). Figure 8 shows the UV/vis spectrum of the thin film of the polymer (Polymer I). The major absorption band around 380 nm is attributed to the absorption of the PPV backbone overlapping with that of the chromophore, which is supported by the similarity of this spectrum with that of the polymer without Ru complexes (Polymer II) as also shown in Figure 2. For polymer II, there is an absorption tail extending beyond 600 nm, which can be assigned to the MLCT absorption of the ruthenium complexes. This extending tail is the most interesting feature because it enables us to photoexcite the polymer mainly through MLCT processes by using a He-Ne laser (i.e. 632.8 nm).
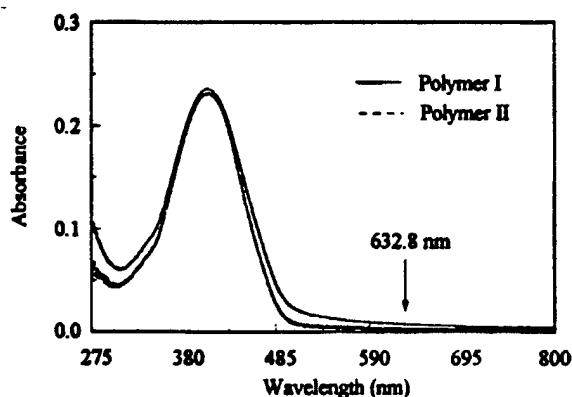

Figure 8. The solid UV/vis spectrum of Polymer I and II.

As we expected, the resulting polymer exhibits a relatively low T_g of 11 ^{0}C, determined by Differential Scanning Calorimetry (DSC). This low Tg and the good solubility in organic solvents make this polymer easy to be processed into high optical quality films of thickness over 100 μm from its solution.

For the purpose of comparison, a neutral conjugated polymer containing a Cu(II)-porphyrin moiety was synthesized with a similar condition (Scheme 13). The resulting polymer (Polymer III) exhibited an M_n of 18 kdalton with a PD of 1.88 determined by GPC. The Tg of the polymer was measured by DSC to be 16 ^{0}C. The structure of the polymer was studied by elemental analysis, ^{1}H NMR and UV/visible absorption spectra. The paramagnetic property of Cu(II) severely broadened the ^{1}H NMR spectra of the monomer and the polymer. In the UV/vis spectrum (in THF), Q bands between 500 and 600 nm could be clearly identified. These results indicate that the metalporphyrin moiety was incorporated into the polymer backbone.

Physical Characterization. A. Photorefractive gain. To study the PR properties of the polymer, the first (also the most important) experiment is the two-beam coupling (2BC) experiment which can determine the PR nature of a material. In this experiment, two coherent laser beams intersect inside of a PR polymer film and a refractive index grating can be generated. Since the phase of the refractive index grating is shifted in comparison to the illumination pattern, the two writing beams are diffracted into each other's direction by these very gratings, accompanied with

asymmetric energy exchange. This feature is cited as the signature of photorefractivity. We performed the 2BC experiment on our polymer film with two p-polarized He-Ne laser beams (632.8 nm) of equal intensity (2x1.6 W/cm^2). The normal of the sample was tilted 52^0 with respect to the bisector of the writing beams in order to provide a projection of the grating wave vector along the poling axis. With this geometry, a holographic grating with a spacing of 2.7 μm was created in the material (refractive index of the polymer at 632.8 nm is 1.63). With the applied field on, clear asymmetric energy transfer between the two beams was observed as shown in Figure 9: one beam gained energy and the other lost energy. As the electric field was turned off, the beam coupling disappeared and the intensities of the both beams returned to their original levels. When the polarity of the applied field was reversed, the gain and loss beams were also switched, as expected, which is due to reversal of the dipole orientation. These experimental results are clear indications that the grating is due to photorefractive effect and not due to thermal or absorption grating.[16] The 2BC gain coefficient (Γ) was calculated according to the following equation:[2(a)]

$$\Gamma = \frac{1}{L} \ln(\frac{1+\alpha}{1-\beta\alpha})$$

where α is the ratio of the intensity modulation (ΔIs/Is) and β is the intensity ratio of the two incident laser beams (Is/Iq).

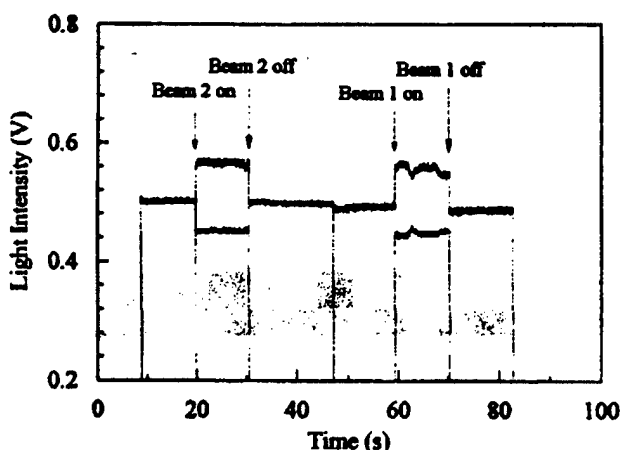Figure 9. Asymmetric energy transfer at the field of 90 V/μm in the 2BC experiment.

B. Local field effect. It is interesting, however, to observe that the optical gain coefficient increases with the external field initially and then levels off when the applied field surpasses about 50V/μm, as shown in Figure 10. This behavior is quite different from those of the low T$_g$ composite PR materials, in which the gain coefficient increases nonlinearly with the applied field. Unlike the high Tg version of this polymer, no net optical gain was observed. At the field of 80 V/μm, an optical gain of 26.6 cm^{-1} was detected, while the absorption coefficient, α, is 28 cm^{-1}.
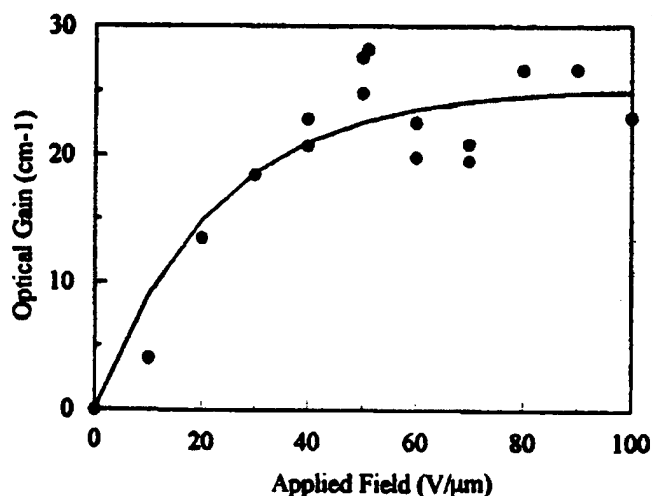
Figure 10. Photorefractive gain coefficient as a function of the applied field.

To understand this deviation in the behavior of field dependence of the 2BC gain coefficient, two necessary elements for the PR effect, photoconductivity and field-induced birefringence (which reflects the E-O effect of the sample), were investigated. The photocurrent and birefringence as a function of the applied field are shown in Figures 11 and 11. The birefringence exhibits typical field enhancement behavior similar to conventional low T_g composite PR polymers,[3,5] while the photocurrent shows the same trend in the field dependence as that of the 2BC gain coefficient: at a field of 50V/μm, the photoconductivity became saturated. It seems that the photoconductive process is the limitation on PR performance.
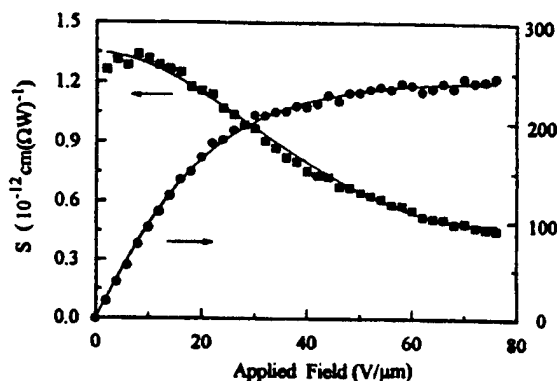

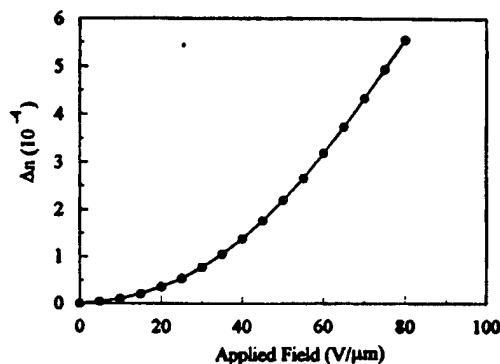Figure 11. Dependence of photoconductive sensitivity on the applied field.

Figure 12. Magnitude of the index and photocurrent modulation versus the applied filed

These results can be attributed to the existence of ionic ruthenium and the low T_g nature of the material. The counterion pairs of PF_6^- and the Ru(II)-tri(bispyridyl) segment form the ionic dipole moment pointing from Ru(II) to $(PF_6^-)_2$. The dipole moment is randomly oriented in the absence of an external field. When an external electric field is applied to the the PR polymer film, the dipoles of both NLO chromophores and the ionic pairs are readily aligned. The effect of alignment of NLO chromophore dipoles on the local field is uniform throughout the film and is

32

limited due to the thermal randomization. This dipole alignment becomes significant for ionic species in a low T_g polymer because of the large freedom of local motion of the polymer chains and the high mobility of the ions, PF_6^-. The magnitude of the ionic dipole moment also increases with the field due to the increase in the distance between the ion-pair and the decrease in the angle between the two sub-dipoles formed by the ionic Ru complex center with two PF_6^- ions which overcomes the repelling force between the two PF_6^- ions. This magnitude change of the dipole with the applied field makes the ion-pair field increases superlinearly in response to the external field. As a result, the higher the external field applied, the stronger the counter internal field generated from the ion dipoles and this counter internal field partially screens Ru(II)-tri(bispyridyl) complex sites from the applied external field.

It is well known that photogeneration of charge carriers in organic polymers involves a two-step mechanism: the photoexcitation and dissociation of the bound electron-hole pair.[17] To assist the separation of the bound pairs, an applied field is always needed. Therefore, the photogeneration efficiency of charge carriers is strongly dependent on the local field around the photocharge generation sites. Since the ruthenium complex acts as a photocharge generator, the screen effect due to this ionic dipole field will reduce the photocarrier separation efficiency and cause the photocurrent to saturate. The photoconductive sensitivity (S) could be estimated from the photocurrent (I_{ph}) by the following expression:[18]

$$S = \frac{I_{ph}L}{AVI_0}$$

where L is the sample thickness, A is the illumination area, V is the applied voltage and I_0 is the intensity of illumination of the beam. As a result of the decrease in photogeneration efficiency of charge carriers, the photoconductive sensitivity decreases as the increase of the applied field.(Figure 11)

According to the 'standard PR theory' developed for inorganic ferroelectric single crystals, the saturation of optical gain can possibly be explained by the decrease of the effective trap density at the high field. But, the decrease in the effective trapping centers should lead to the increase of the photoconductive sensitivity with the external field.[19] This is clearly in contrast with our experimental results that the photoconductive sensitivity decreased dramatically with the increase of the external field (Figure 11). The most reasonable explanation must be that the dipole field induced by ion-pairs limits charge generation rate and further the steady-state space-charge field. Unfortunately, the 'standard PR theory' does not predict the relationship of the space-charge field with the charge generation rate.[20] This theory was obtained under many simplified assumptions, especially under the condition that no thermal and electric-induced detrapping occurs after the trapping of the carrier. In reality, organic PR materials, especially for those low T_g materials, the trapped charge could be more easily detrapped than that in inorganic PR materials because of the amorphous nature. If the detrapping rate is large enough, the condition that space-charge fields being limited by trap density could never be reached and the space-charge field would be a function of photoconductivity.[21] The PR optical gain therefore became saturated at high field.

This screen effect was also reflected in degenerate four-wave mixing (DFWM) experiments. In this experiment, the two s-polarized beams (632.8 nm, 2x1.45 W/cm^2) were used as writing beams and the grating formed in the material was read out with a weak p-polarized reading beam (632.8 nm, 230 mW/cm^2) counter-propagating to one of the writing beams. The diffraction efficiency, η, defined as the ratio of the diffracted to incident reading beam power, was recorded. Because the diffraction efficiency is determined by the amplitude of the index grating, a similar

behavior to the optical gain is expected if the index grating is formed mainly due to the photorefractive effect. As shown in Figure 8, the value of η increased with the applied field and became saturated at 0.5% at the field of 50 V/μm. When the pump beam was blocked, the diffracted signal dropped immediately.

The spacing of the space-charge field in the 2BC experiment is about 2.7 μm, which is more than three orders of magnitude larger than the diameter of the polymer backbone. Therefore, this internal field induced by ionic dipole moment is a local effect compared to the variation of the space-charge field. Because the Ru(II)-tri(bispyridyl) complex is only 1 mol% in the polymer system, large amounts of the segments with the NLO chromophore are not influenced by this local internal field. Therefore, the birefringence due to the alignment of the dipole moments of the NLO chromophores and Pockel effect, should not exhibit any saturation. This is indeed the case as shown in Figure 12. Second harmonic generation (SHG) experiments indicate a field dependent behavior of the SHG signal similar to most of the NLO polymers. The NLO chromophores could be effectively aligned at room temperature by applying an external field and the effect of the ionic dipole field was not observed.(Figure 13).
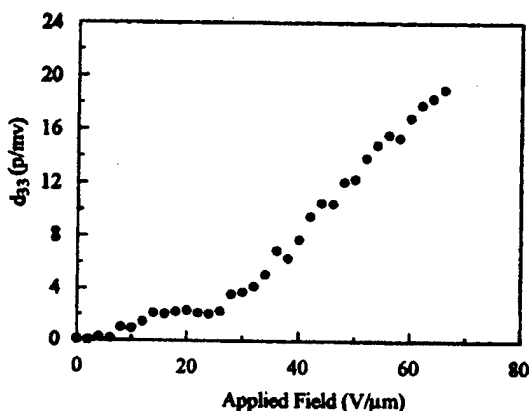

Figure 13. d33 vs applied field.

Although the internal field induced by the ion dipole limits the PR performance in our low Tg materials, this limitation should not present in high Tg materials since the local motion of the polymer chain is so small that the ion dipole cannot be effectively aligned by the applied field at room temperature. In fact, the photocarrier separation and mobility at zero external field could be further enhanced by the internal field produced by the aligned ion pairs and the dipoles of NLO chromophores in PR polymer films after corona poling at an elevated temperature. It seems to us that the enhancement of photoconductivity and the stability of the aligned NLO chromophore are responsible for the extraordinary large PR optical gain at zero field in our previous reported PR polymer that contains an ionic Ru(II)-tri(bispyridyl) complex and possesses a Tg as high as 130 ^{0}C.[13]

C. The dynamics of grating formation. The dynamics of holographic grating formation was studied by measuring the time constants of the grating formation and their electric field dependence in the DFWM experiment. A typical behavior of grating formation is illustrated in Figure 14, in which the writing beams are turned on at time t = 0. A fast initial rise in the diffraction signal is observed, which slows and saturates after approximately 70-s writing time. The rapid initial rise accounts for about 80% of the saturated value of diffraction efficiency. Quantitative information about the grating growth can be obtained by an empirical two-exponential fit of the following form to the data of diffraction intensity:

$$\eta(t) \sim \{E_{scf}[1-\exp(-t/\tau_f)]+E_{scs}[1-\exp(-t/\tau_s)]\}^2$$

where E_{scf}, E_{scs}, τ_f, τ_s are the four fitting parameters. The fast component of the diffraction efficiency is indicated by the first term of the equation, while the slow component is represented by the second term of the equation. Figure 15 shows the dependence of the initial grating growth rate and the slow rate on the applied field. High electric field markedly increases the speed of the initial grating formation (Figure 15a). At the field of 80 V/μm, the initial grating writing time constant is around 0.21 s, which is comparable with that of the fastest known PR polymers. Such a fast response time may be attributed to large charge carrier mobility and facile NLO chromophore alignment in this type of material. It was known that there are many different mechanisms that contribute to photoconductivity and photorefractive charge storage.[22] Since the charge transporting processes in organic amorphous materials are usually very dispersed, the formation of space-charge field does not bear an exponential relationship to the photoconductivity. In our polymer, although the screening from the ion pairs limited the photocharge generation efficiency, the transporting of charge carriers is not affected since the ion-pair field is still a local effect comparing to the drift length, which is typically in the order of submicron. The mobility of the charge carriers -- the hopping process -- can still be greatly enhanced by the applied field. Therefore, the initial space-charge field could be formed through certain fast carrier transporting channels without the limitation by the carrier generation rate. The behavior of the slow rate is interesting and reflects the effect of the ionic dipole field on the photogeneration rate of the charge carriers (Figure 15 b). Then the formation speed slows down because of the limitation on the photocharge generation, and makes the slow component almost independent of the applied field at high external field (Fig. 15(b)).
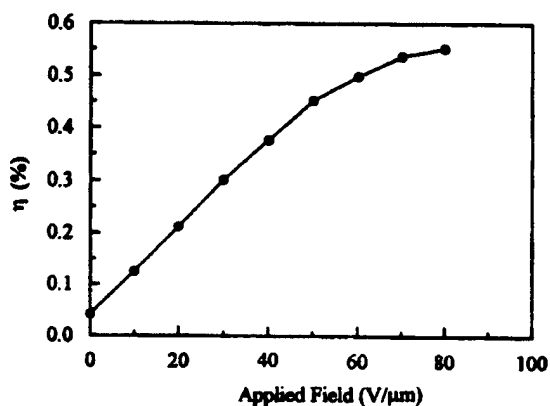

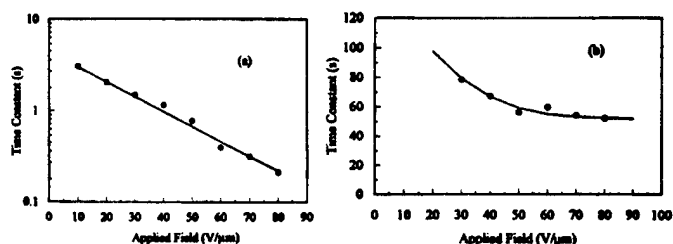Figure 14. Diffraction efficiency VS field.

Figure 15 a and B: Response time Vs field

a: Fast component; b. Slow component.

Conclusions

A novel low T_g PR polymer which contains tri(bispyridyl) ruthenium(II) as photosensitizer has been synthesized. Its PR properties have been studied through the analyses of the dependence of photoconductivity, optical gain coefficient, birefringence, E-O activities, and diffraction efficiency on the field. It was found that the ionic dipole moments in this low T_g ionic PR polymer are easily aligned and generate an internal field to screen the photocharge generation site from the external applied field. Such screen effect limits the photocharge generation efficiency and PR performance at high applied field. A saturation was observed in the field dependence of photoconductivity, PR optical gain coefficient and diffraction efficiency. We believe that this investigation of the local

field effect on photocharge generation should be useful enlightenment for development and optimization new PR polymer. The above results indicate that to synthesize a high performance PR polymers, a low T_g PR polymer containing neutral Ru complexes should be explored to fully utilize the efficient MLCT process and orientational enhancement.

Experimental Section

Tetrahydrofuran (THF) and ethyl ether were purified by distillation over sodium chips and benzophenone. The *p*-divinylbenzene was separated from a mixture of *p*-divinylbenzene and *m*-divinylbenzene according to the literature procedure.[23] All of the other chemicals were purchased from Aldrich Chemical Co. and used as received unless otherwise noted. Compound **3** and monomer C were prepared according to the ref. 13 and 24.

Synthesis of Monomers: Compound 2. To the nickel catalyst prepared from $NiBr_2(PPh_3)_2$ (14.38 g, 19.35 mmol), zinc (6.33 g, 96.83 mmol) and Et_4NI (16.60 g, 64.55 mmol) in THF (90 mL), was added a solution of 11.1 g (64.5 mmol) of 2-bromo-5-picoline (**1**) in THF (40 mL). After stirring at 50 °C for 20 h, the mixture was poured into 2M aqueous ammonia (500 mL), followed by addition benzene (250 mL) and ethyl acetate (250 mL). A brown cloudy solution was given. After filtration, the filtrate was extracted with benzene/AcOEt (1:1). The organic layer was washed with water, dried over anhydrous $MgSO_4$ and evaporated in vacuo. The residue was separated by flash chromatography (silica gel, benzene/AcOEt (10:1)) to give 5,5'-Dimethyl 2,2'-bipyridine (**2**) (4.3 g, 73%). ^1H NMR ($CDCl_3$, ppm): δ 2.35 (s, 6H, $-CH_3$), 7.61 (d, $J = 8.08$ Hz, 2H, aromatic protons), 8.24 (d, $J = 8.09$ Hz, 2H, aromatic protons), 8.49 (s, 2H, aromatic protons).

Compound 5. 1-Bromodecane (22.92 g, 0.1035 mol) in 18 mL ether was added to a suspension containing Mg (2.5 g, 0.1028 mol) and ether (25 mL) at a rate to maintain the refluxing of the reaction mixture. After the addition was complete, the mixture was further heated to reflux for half an hour. The solution was then added dropwise into a mixture containing 1,4-dibromobenzene (**4**) (11.0 g, 0.0466 mol), $PdCl_2(dppf)$ (0.76 g, 0.93 mmol), and 40 mL ether. The resulting mixture was refluxed overnight and then poured into water. After removal of the catalyst residue (red precipitate) by filtration, the filtrate was extracted with ether. The combined organic layer was then washed with water and dried by $MgSO_4$. Evaporation of the solvent gave a brown oil which was distilled under vacuum, yielding a slight yellow oil.(14.19 g, 85%, bp 213-214 °C at 0.2 mmHg) ^1H NMR ($CDCl_3$, ppm): δ 0.87 (t, $J = 6.58$ Hz, 6H, $-CH_3$), 1.25-1.29 (m, 32H, alkyl protons), 1.57 (m, 4H, alkyl protons), 2.55 (t, $J = 7.81$ Hz, 4H, benzyl protons), 7.07 (s, 4H, aromatic protons).

Compound 6. A mixture of compound **5** (11.48 g, 0.032 mol), iodine (10.17 g, 0.04 mol), H_5IO_6 (3.8 g, 0.017 mol), acetic acid (30 mL), 30% sulfuric acid (15 mL) and chloroform (15 mL) was stirred at 80 °C for 48 h and then poured into water. The crude product was collected by filtration and washed with water and cold ethanol. Recrystallization from ethanol/ethyl acetate (6:1) gave a colorless solid.(14.66 g, 75%) ^1H NMR ($CDCl_3$, ppm) δ 0.88 (t, $J = 6.58$ Hz, 6H, $-CH_3$), 1.27-1.35 (m, 28H, alkyl protons), 1.52-1.57 (m, 4H, alkyl protons), 2.59 (t, $J = 7.81$ Hz, 4H, benzyl protons), 7.59 (s, 2H, aromatic protons).

Compound 7. *n*-BuLi (3.8 mL, 2.5 M solution in hexane, 9.424 mmol) in 15 mL ether was added dropwise in the 35 mL ether solution of compound **6** (5.75 g, 9.425 mmol) at 0 °C. After the addition of BuLi was completed, DMF (1.09 mL, 14.13 mmol) in 5 mL ether was added dropwise into the solution. The resulting mixture was stirred at room temperature for 2 h and poured into water. The organic layer was collected and the aqueous layer was extracted with ether. The

combined organic layer was washed with water and dried over MgSO$_4$. After removal of the solvent, the crude product was chromatographed (silica gel, hexane/ethyl acetate (20:1)) to give a colorless solid.(3.37 g, 70%) ^{1}H NMR (CDCl$_3$, ppm) δ 0.88 (t, J = 6.59 Hz, 6H, -CH$_3$), 1.26-1.35 (m, 28H, alkyl protons), 1.58 (m, 4H, alkyl protons), 2.71 (t, J = 8.03 Hz, 2H, benzyl protons), 2.88 (t, J = 7.99 Hz, 2H, benzyl protons), 7.59 (s, 1H, aromatic protons ortho to CHO), 7.75 (s, 1H, aromatic protons meta to CHO), 10.21 (s, 1H, -CHO).

Compound 8. Sodium hydride (0.37 g, 15.42 mmol) was added to a solution of compound 7 (5.27 g, 10.29 mmol) in 25 mL 1,2-dimethoxyethane (DME). The resulting suspension was stirred for 10 min. at room temperature. Compound 3 (2.35 g, 5.15 mmol) in DME (10 mL) was then added dropwise. The mixture was refluxed overnight. After the solution cooled down to room temperature, water and dichloromethane were added. The crude product was precipitated out and separated by filtration. Recrystallization from dichloromethane gave a bright yellow solid of compound **8.**(5.07 g, 84%) ^{1}H NMR (CDCl$_3$, ppm) δ 0.85-0.89 (m, 12H, -CH$_3$), 1.25-1.55 (m, 56H, alkyl protons), 1.69 (m, 8H, alkyl protons), 2.64-2.72 (m, 8H, benzyl protons), 7.05 (d, J = 16.14 Hz, 2H, vinyl protons), 7.39 (d, J = 16.12 Hz, 2H, vinyl protons), 7.44 (s, 2H, aromatic protons meta to I), 7.64 (s, 2H, aromatic protons ortho to I), 7.98 (d, J = 8.38 Hz, 2H, 4-pyridine protons), 8.43 (d, J = 8.30 Hz, 2H, 3-pyridine protons), 8.79 (s, 2H, 6-pyridine protons). Anal. Calcd for C$_{66}$H$_{98}$N$_2$I$_2$: C, 67.60; H, 8.36; N, 2.39. Found: C, 67.41; H, 8.30; N, 2.40.

Monomer A. A solution of compound 8 (0.306 g, 0.261 mmol), cis-dichlorobis(2,2'-bipyridine)ruthenium(II) hydrate (0.126 g, 0.261 mmol) and 25 mL methoxyethanol was stirred at 140 °C for 4 h. After cooling to room temperature, the solution was added into an (NH$_4$)PF$_6$ (0.425 g, 2.61 mmol) aqueous solution. The solid precipitated out and was purified by chromatography (silica gel, dichloromethane/methanol (20:1)).(0.274 g, 56%) ^{1}H NMR (CDCl$_3$, ppm) δ 0.85 (t, J = 6.54 Hz, 12H, -CH$_3$), 1.18-1.48 (m, 64H, aliphatic protons), 2.53-2.64 (m, 8H, benzyl protons), 6.79 (d, J = 16.42 Hz, 2H, vinyl protons), 7.30 (d, J = 16.42 Hz, 2H, vinyl protons), 7.42 (s, 2H, aromatic protons meta to iodo), 7.46 (m, 4H, aromatic protons), 7.56 (s, 2H, aromatic protons ortho to iodo), 7.63 (s, 2H, aromatic protons), 7.76 (dd, J = 5.10 Hz, 4H, aromatic protons), 7.95 (d, J = 8.37 Hz, 4H, aromatic protons), 8.38 (d, J = 8.79 Hz, 2H, aromatic protons), 8.41 (m, 6H, aromatic protons). Anal. Calcd for C$_{86}$H$_{114}$N$_6$I$_2$P$_2$F$_{12}$Ru: C, 55.04; H, 6.07; N, 4.48; I, 13.52. Found: C, 55.06; H, 6.09; N, 4.47; I, 13.60.

Compound 9 was obtained from 1.4-dibromobenzene (4) in 78% yield, following a procedure similar to that described for compound 5. ^{1}H NMR (CDCl$_3$, ppm) δ 0.88 (t, J = 6.70 Hz, 3H, -CH$_3$), 1.28 (m, 26H, alkyl protons), 1.57 (m, 2H, alkyl protons), 2.55 (t, J = 7.60 Hz, 2H, benzyl protons), 7.05 (d, J = 8.30 Hz, 2H, aromatic protons), 7.38 (d, J = 8.30 Hz, 2H, aromatic protons).

Compound 10. Compound 9 (7.18 g, 18.8 mmol) in 20 mL THF was added dropwise into a mixture of Mg (0.55 g, 22.2 mmol), 10 mL THF and a small crystal of iodine at such a rate that the reaction mixture maintained self-refluxing. After the addition was complete, the mixture was heated to reflux for half an hour. The resulting Grignard reagent was transferred by a needle to a mixture containing 1.12-dibromododecane (9.25 g, 28.18 mmol), Li$_2$CuCl$_4$ (2.8 mL of 0.1 M THF solution, 28.18 mmol) and 20 mL THF. The resulting mixture was stirred overnight at room temperature and then poured into water. The mixture was extracted with dichloromethane. The combined organic layer was washed successively with saturated aqueous NaHCO$_3$ solution, water and dried over MgSO$_4$. The solvent was removed by rotary evaporation, and the residue was recrystallized from

acetone to give a colorless solid of compound **10**.(6.71 g, 65%) ^{1}H NMR (CDCl$_3$, ppm) δ 0.87 (t, J = 6.59 Hz, 3H, -CH$_3$), 1.25-1.29 (m, 40H, alkyl protons), 1.38 (m, 2H, alkyl protons), 1.55 (m, 4H, alkyl protons), 1.85 (m, 2H, alkyl protons), 2.58 (t, J = 7.65 Hz, 4H, benzyl protons), 3.41 (t, J = 6.88 Hz, 2H, -CH$_2$Br), 7.08 (s, 4H, aromatic protons).

Compound 11 was obtained from compound **10** in 60% yield, following a procedure similar to that described for compound **6**. ^{1}H NMR (CDCl$_3$, ppm) δ 0.87 (t, J = 6.60 Hz, 3H, -CH$_3$), 1.26-1.32 (m, 40H, alkyl protons), 1.39 (m, 2H, alkyl protons), 1.55 (m, 4H, alkyl protons), 1.85 (m, 2H, alkyl protons), 2.59 (t, J = 7.82 Hz, 4H, benzyl protons), 3.41 (t, J = 6.85 Hz, 2H, -CH$_2$Br), 7.59 (s, 2H, aromatic protons).

Compound 12. A mixture of compound **11** (4.13 g, 5.15 mmol), N-ethyl aniline (1.30 mL, 10.31 mmol), potassium carbonate (2.14 g, 15.48 mmol), tetrabutylammonium bromide (0.166 g, 0.515 mmol) and sodium iodine (7 mg, 0.047 mmol) in toluene (12 mL) was refluxed overnight. The mixture was then poured into water and extracted with dichloromethane. The organic layer was separated and washed with water, dried over MgSO$_4$. After the solvent was evaporated, the residue was purified by flash chromatography (silica gel, hexane/dichloromethane (2:1)).(3.37 g, 78%) ^{1}H NMR (CDCl$_3$, ppm) δ 0.88 (t, J = 6.58 Hz, 3H, -CH$_3$), 1.14 (t, J = 7.04 Hz, 3H, -NCH$_2$CH$_3$), 1.22-1.31 (m, 42H, alkyl protons), 1.54 (m, 6H, alkyl protons), 2.58 (t, J = 7.83 Hz, 4H, benzyl protons), 3.24 (t, J = 7.63 Hz, -CH$_2$N-), 3.34 (quintet, J = 7.04 Hz, 2H, -NCH$_2$CH$_3$), 6.64 (m, 3H, aromatic protons), 7.20 (t, J = 7.24 Hz, 2H, aromatic protons), 7.59 (s, 1H, aromatic protons).

Compound 13. To a ice-cooled DMF (2 mL, 25.83 mmol) phosphorous oxychloride (0.762 g, 4.96 mmol) was added dropwise. The solution was stirred at 0 °C for 1 h and at room temperature for another 1 h. Compound **12** (3.8 g, 4.517 mmol) in 7 mL DMF was then added dropwise to the mixture and the resulting solution was stirred at 90 °C overnight. The solution was poured into water and extracted with dichloromethane. The separated organic layer was washed with water and dried. After the solvent was evaporated, the residue was chromatographed (silica gel, hexane/ethyl ether (2:1)) to give a colorless liquid.(2.40 g, 61%) ^{1}H NMR (CDCl$_3$, ppm) δ 0.88 (t, J = 6.53 Hz, 3H, -CH$_3$), 1.18-1.33 (m, 45H, alkyl protons), 1.61 (m, 6H, alkyl protons), 2.58 (t, J = 7.73 Hz, 4H, benzyl protons), 3.25 (t, J = 7.60 Hz, -CH$_2$N-), 3.32 (quintet, J = 7.01 Hz, 2H, -NCH$_2$CH$_3$), 6.67 (d, J = 8.44 Hz, 2H, aromatic protons), 7.59 (s, 1H, aromatic proton), 7.72 (d, J = 8.44 Hz, 2H, aromatic protons), 9.69 (s, 1H, -CHO).

Monomer B. Sodium hydride (0.145 g, 6.04 mmol) was added to a solution of compound **13** (2.91 g, 3.348 mmol) in 10 mL DME. The suspension was stirred for 10 min. at room temperature, followed by dropwise addition of the solution of diethyl 4-(hexylsulfone)benzyl phosphate (1.26 g, 3.348 mmol) in 5 mL DME. The resulting solution was stirred at 80 °C overnight and then poured into water. The mixture was extracted with dichloromethane. The combined organic layer was washed with water and dried. After removal of the solvent, the residue was separated by chromatography (silica gel, hexane/ethyl ether (4:1)) to give a greenish yellow solid.(1.756 g, 48%) ^{1}H NMR (CDCl$_3$, ppm) δ 0.87 (m, 6H, -CH$_3$), 1.17-1.69 (b, 59H, alkyl protons), 2.58 (t, J = 7.63 Hz, 4H, benzyl protons), 3.07 (t, J = 8.14 Hz, 2H, -SO$_2$CH$_2$-), 3.23 (t, J = 7.31 Hz, 2H, -CH$_2$N-), 3.35 (quintet, J = 6.85 Hz, 2H, -NCH$_2$CH$_3$), 6.64 (d, J = 8.82 Hz, 2H, aromatic protons), 6.85 (d, J = 16.20 Hz, 1H, vinyl proton), 7.12 (d, J = 16.15 Hz, 1H, vinyl proton), 7.40 (d, J = 8.73 Hz, 2H, aromatic protons), 7.59 (m, 4H, aromatic protons), 7.80 (d, J = 8.40 Hz, 2H, aromatic protons). Anal. Calcd for C$_{56}$H$_{87}$SNI$_2$O$_2$: C, 61.58; H, 7.96; N, 1.28. Found: C, 61.65; H, 7.98; N, 1.23.

Polymerization. A typical polymerization procedure is following: Tri-n-butylamine (0.32 mL, 1.34 mmol) was added to the mixture of monomer **A** (0.010g, 0.00540 mmol), monomer **B** (0.5890g, 0.5400 mmol), p-divinylbenzene (0.070g, 0.545 mmol), palladium acetate (4.9 mg, 0.0217 mmol) and tri-o-tolyphosphine (32.9 mg, 0.108 mmol) in 5 mL DMF. The reaction mixture was stirred at 90 $^\circ$C overnight under a nitrogen atmosphere and then poured into methanol. The precipitate was collected, redissolved in chloroform and filtered to remove the catalyst residue. The filtrate was concentrated and precipitated into methanol followed again by filtration, reprecipitation. The resulting polymer was further purified by extraction in a Soxhlet extractor with methanol for 24h and then was dried under a vacuum at 40 $^\circ$C for 24h.

Polymer I: Anal. Calcd for $C_{66.3}H_{95.27}N_{1.05}O_{1.98}S_{0.99}P_{0.02}F_{0.12}Ru_{0.01}$: C, 81.79; H, 9.78; N, 1.51; Ru, 0.10. Found: C, 81.07; H, 9.87; N, 1.41; Ru, 0.08.

Polymer II: Anal. Calcd for $C_{66}H_{95}NO_2S_1$: C, 82.08; H, 9.84; N, 1.45. Found: C, 81.90; H, 9.92; N, 1.31.

Polymer III: Anal. Calcd for $C_{66.54}H_{15.68}N_{1.04}O_2SCu_{0.01}$: C, 82.04; H, 9.82; N, 1.49. Found: C, 81.41; H, 9.57; N, 1.44.

Characterization. The ^{1}H NMR spectra were collected on a Bruker 500-MHz FT NMR spectrometer. A Shimadzu UV-2401PC UV/Vis was used to record the UV/Vis spectra. Thermal analyses were performed by using the DSC-10 system from TA Instruments with a heating rate of 10 $^\circ$C/min under a nitrogen atmosphere. Elemental analyses were performed by Atlantic Microlab, Inc., except for the ruthenium analyses, which were done by Galbraith Laboratories, Inc.. Molecular weights were measured with a Water RI GPC system using polystyrene as the standard and THF as the eluent.

The films for PR characterization were made by sandwiching polymers between two indium-tin-oxide (ITO) covered glass substrate. The thickness of the film was fixed around 104 μm with the help of polyimide spacers.

The photoconductivity measurements were performed on about 26 μm thick film sandwiched between Au and ITO electrodes at a wavelength of 632.8 nm using a photocurrent method.[25] The photocurrent was measured by monitoring the voltage drop on a resistor which is in series with the film capacitor.

Second-order NLO properties of polymeric films were characterized by second harmonic generation experiment. A mode-lock Nd:YAG laser (Continuum-PY 61 C-10, 10-Hz repetition rate) was used as the light source. The second harmonic of the fundamental wave (1064 nm) generated by the polymer sample was detected by a photomultiplier (PMT) and then amplified and averaged in a boxcar integrator. The d_{33} value was obtained by assuring $d_{33} = 3d_{31}$ with a quartz crystal as the reference sample.

The electric field induced birefringence was measured using an ellipsometric method with a crossed-polarizer geometry on the same sample as in PR measurements.[26] The sample normal was titled at 45 $^\circ$C with respect to the incident light. The polarization of the incident light was 45 $^\circ$C with respect to the incident plane.

Two-beam coupling experiments were performed using a He-Ne laser (632.8 nm, 30 mW) as the light source. The laser beam (p-polarized) was split into two beams with equal intensity (2×1.6 W/cm^2), which were intersected in the polymer film at 24.5 $^\circ$C. The transmitted intensities of the two beams were monitored by two diode detectors and the data were recorded by a computer.